

Copy  
RM L53H31

THIS DOCUMENT AND EACH AND EVERY  
PAGE HEREIN IS HEREBY RECLASSIFIED

FROM CONF TO UNCLASSIFIED,  
AS PER LETTER DATED DEC 1953  
ALL #115 (OCB)

L.E. CH. EXT.  
NOTCH  
GLOVE

NACA

WBVH

# RESEARCH MEMORANDUM

SOME LOW-SPEED WIND-TUNNEL EXPERIMENTS PERTAINING TO  
THE LONGITUDINAL STABILITY CHARACTERISTICS  
OF A 35° SWEPT-WING MODEL AND AN  
UNSWEPT-WING MODEL

By Byron M. Jaquet

Langley Aeronautical Laboratory  
Langley Field, Va.

ENGINEERING DEPT. LIBRARY  
CHANCE-VOUGHT AIRCRAFT  
DALLAS, TEXAS

CLASSIFIED DOCUMENT

This material contains information affecting the National Defense of the United States within the meaning  
of the espionage laws, Title 18, U.S.C., Sections 793 and 794, the transmission or revelation of which in any  
manner to an unauthorized person is prohibited by law.

NATIONAL ADVISORY COMMITTEE  
FOR AERONAUTICS

WASHINGTON

October 20, 1953

NATIONAL ADVISORY COMMITTEE FOR AERONAUTICS

RESEARCH MEMORANDUM

SOME LOW-SPEED WIND-TUNNEL EXPERIMENTS PERTAINING TO  
THE LONGITUDINAL STABILITY CHARACTERISTICS  
OF A  $35^{\circ}$  SWEPT-WING MODEL AND AN  
UNSWEPT-WING MODEL

By Byron M. Jaquet

SUMMARY

An investigation has been conducted in the Langley stability tunnel to determine the effects of various leading-edge flow-control notches and associated devices, horizontal-tail span, wing sweep, aspect ratio of an unswept wing, and horizontal-tail position on the static longitudinal stability characteristics of an airplane model having swept tail surfaces.

Of the single leading-edge flow-control notches investigated a 2-percent-semispan notch at 74-percent semispan from the plane of symmetry had the best over-all stability characteristics, although the notch did not provide better than neutral stability where the original swept-wing model was unstable (plain flaps neutral or deflected). Various changes in this notch, including reducing the span, had a detrimental effect on the effectiveness of the notch in reducing the pitch-up. A comparison of the effects of a chordwise fence, a chord-extension, and the best notch on the static longitudinal stability characteristics of the model indicated that the chord-extension was the most favorable device since the region of neutral stability was the smallest. The fence and notch arrangements had about the same longitudinal stability characteristics.

A decrease in aspect ratio of the unswept wing from 3.57 to 2.50 had little effect on the longitudinal stability of the model. However, a further decrease in aspect ratio to 1.00 resulted in a pitch-up at a low lift coefficient which became more severe as the aspect ratio was decreased. For the aspect-ratio-2.50 unswept-wing model, lowering the horizontal tail had a detrimental effect on the stability of the model at low angles of attack since the tail apparently moved into the wing wake.

## INTRODUCTION

Various devices consisting of chordwise fences, leading-edge chord-extensions, and drooped leading-edge and chord-extension combinations have been employed in an attempt to eliminate the undesirable pitch-up characteristics exhibited at low angles of attack by a  $35^{\circ}$  swept-wing airplane model in the wind-tunnel investigations reported in references 1 to 3. The investigation of reference 2 indicated that this pitch-up was the result of a rapid increase in the rate of change of downwash at the horizontal tail with angle of attack, this rapid change of downwash being caused by the inboard movement of the leading-edge separation vortex as the angle of attack is increased. The use of a chordwise fence (a physical barrier to the vortex) or a chord-extension (primarily providing an aerodynamic barrier to the vortex) improved the stability although neither device resulted in better than neutral stability in the angle-of-attack range where the pitch-up occurred for the original swept-wing model.

In view of the improvement in stability caused by the chordwise fence, flight tests were made with a chordwise fence installed on the full-scale airplane (ref. 4). Although the wind-tunnel tests (ref. 1) indicated a large improvement in stability from severe pitch-up to neutral stability, the flight tests (ref. 4) indicated only minor effects of the fence on the pitch-up of the full-scale airplane. This is a further indication that, in order to eliminate the pitch-up of a full-scale airplane, a fix may have to provide more than neutral static longitudinal stability. (See ref. 5.)

The present exploratory investigation was made in the Langley stability tunnel to determine the effects of various leading-edge flow-control notches, leading- and trailing-edge extensions, and horizontal-tail span on the low-speed static longitudinal instability (pitch-up) of a  $35^{\circ}$  swept-wing airplane model. In order to provide information on the effects of decreasing the vortex span of an unswept wing on the longitudinal stability of a model having the same fuselage-tail combination as the swept-wing model, an unswept wing with the aspect ratio varying from 3.57 to 1.00 was investigated. The aspect ratio of the wing was varied by cutting portions from the tips to provide aspect ratios of 3.00, 2.50, 2.25, 2.00, 1.50, and 1.00. The effect of horizontal-tail position on the stability was determined for the aspect-ratio-2.50 wing-fuselage combination.

## SYMBOLS

The data presented herein are in the form of standard NACA symbols and coefficients of forces and moments and are referred to the stability system of axes with the origin at the projection of the quarter-chord

point of the mean aerodynamic chord of the original swept wing on the plane of symmetry. The positive direction of the forces, moments, and angular displacements is shown in figure 1. The coefficients of the unswept wings were based on the geometry for the respective aspect ratio. The coefficients, which were based on the geometry of the original swept wing, and symbols used herein are defined as follows:

$C_L$	lift coefficient, $L/qS$
$C_{L_{\max}}$	maximum lift coefficient
$C_D$	drag coefficient, $D/qS$
$C_m$	pitching-moment coefficient, $M/qS\bar{c}$
$L$	lift, lb
$D$	drag, lb
$M$	pitching moment, ft-lb
$A$	aspect ratio, $b^2/S$
$b$	wing span, ft
$b_H$	horizontal tail span, ft
$S$	wing area, sq ft
$c$	wing local chord parallel to plane of symmetry, ft
$\bar{c}$	wing mean aerodynamic chord, $\frac{2}{S} \int_0^{b/2} c^2 dy$ , ft
$c_t$	tip chord, ft
$c_r$	root chord, ft
$\lambda$	taper ratio, $c_t/c_r$
$y$	spanwise distance measured perpendicular to plane of symmetry, ft

$q$	dynamic pressure, $\frac{\rho V^2}{2}$ , lb/sq ft
$\rho$	density of air, slug/cu ft
$V$	free-stream velocity, fps
$i_w$	incidence of wing-root chord line with respect to fuselage center line, deg ( $3^\circ$ for present investigation)
$\alpha$	angle of attack of fuselage center line, deg
$\alpha_w$	angle of attack of wing-root chord line, deg
$\delta_f$	deflection of plain trailing-edge flaps, deg (measured perpendicular to hinge line)
$\Lambda$	angle of sweep of 0.333 chord line, deg

#### APPARATUS, MODELS, AND TESTS

The present investigation was conducted in the 6-foot-diameter test section of the Langley stability tunnel with the model mounted at the origin of the axis system on a single support strut. The support strut was attached to a six-component balance system.

Details of the original swept-wing model used in the present investigation are shown in figure 2. The original swept wing had an aspect ratio of 3.57, a taper ratio of 0.565, an area of 2.975 square feet, and a mean aerodynamic chord of 0.942 feet. Also shown in figure 2 are the various horizontal-tail spans investigated. The smallest tail span was 0.696 of the original tail span.

The various single leading-edge flow-control notch arrangements investigated are shown in figure 3 and the multiple-notch arrangements and the notch and sharp-leading-edge chord-extension arrangements investigated are shown in figure 4. The notch and trailing-edge extension combinations and notch and airfoil-shaped leading-edge chord-extension combination investigated are shown in figure 5. Table I summarizes the notch geometry. The various configurations will be referred to hereafter by the number given in table I. Details of fence A of reference 1 and its chordwise location and a typical section through the plain trailing-edge flap and sharp leading-edge extension are shown in figure 6.

The unswept wings used in the investigation are shown in figure 7. The unswept wing of aspect ratio 3.57 had the same plan form, trailing-edge angle, and thickness ratio as the swept wing. For constructional simplicity, a modified flat-plate airfoil section with a rounded leading edge and beveled trailing edge was used. The position of the unswept wings on the fuselage is indicated in figure 2 by the dotted plan form which represents the unswept wing of aspect ratio 3.57. The aspect ratio was varied from 3.57 to 1.00 by cutting portions from the tips. The original horizontal-tail position was used for these wings. Two additional horizontal-tail positions investigated with the aspect-ratio-2.50 unswept wing are also shown in figure 2. These positions were previously used with the swept wing (ref. 6).

The force tests, consisting of the measurement of lift, drag, and pitching moment through an angle-of-attack range of about  $0^\circ$  to  $28^\circ$ , were made at a dynamic pressure of 39.7 pounds per square foot. The test Mach number was 0.17 and the Reynolds number was  $1.1 \times 10^6$  based on the mean aerodynamic chord of the plain wing. A few tests were made with the horizontal tail removed and with the plain trailing-edge flaps deflected  $50^\circ$ . Landing gear and doors were not used for the present tests.

Surface tuft photographs were taken for the original swept-wing model (configuration 1) and with a  $0.02b/2$  notch with the inboard edge at  $0.74b/2$  (configuration 12) from the plane of symmetry. The tufts were located along the following chord lines: 0.05, 0.15, 0.25, 0.35, 0.45, and 0.55. The Reynolds number for these tests was  $0.885 \times 10^6$  and the dynamic pressure was 24.9 pounds per square foot.

#### CORRECTIONS

Approximate jet-boundary corrections, based on unswept-wing concepts, have been applied to the angle of attack and the drag coefficient. The methods of reference 7, also for unswept wings, were used to determine blockage corrections which were applied to the drag coefficient and dynamic pressure. Jet-boundary corrections were applied to the horizontal-tail-on pitching moments and were determined by the methods of reference 8.

Support strut-tares have not been applied to the data but, with the exception of the drag tare, are on the basis of past experience believed to be small. The absolute values of the drag coefficient are not believed to be representative of free-air conditions; however, the increments due to the notches and the changes in tail position and aspect ratio of the unswept wing are believed to be reliable.

## RESULTS AND DISCUSSION

## Presentation of Data

The figures listed in the following table summarize the results of the present investigation:

	<u>Figure</u>
Effect of spanwise location of $0.02b/2$ notch on aerodynamic characteristics in pitch; $\Lambda = 35^\circ$ ; $\delta_f = 0^\circ$ . . . . .	8
Effects of span of notches and variations of notches on aerodynamic characteristics in pitch; $\Lambda = 35^\circ$ ; $\delta_f = 0^\circ$ . . . . .	9
Effect of closing notch leading edge and multiple-notch arrangement on aerodynamic characteristics in pitch; $\Lambda = 35^\circ$ ; $\delta_f = 0^\circ$ . . . . .	10
Effect of span and chord of wing-fuselage juncture notches on aerodynamic characteristics in pitch; $\Lambda = 35^\circ$ ; $\delta_f = 0^\circ$ . . . . .	11
Effect of sharp leading-edge extensions in combination with a $0.02b/2$ notch at $0.74b/2$ on aerodynamic characteristics in pitch; $\Lambda = 35^\circ$ ; $\delta_f = 0^\circ$ . . . . .	12
Effect of various leading- and trailing-edge extensions on aerodynamics characteristics in pitch; $\Lambda = 35^\circ$ ; $\delta_f = 0^\circ$ . . . . .	13
Aerodynamic characteristics in pitch of a $35^\circ$ swept-wing model with and without a $0.02b/2$ notch at $0.74b/2$ ; horizontal tail on and off; $\delta_f = 0^\circ$ . . . . .	14
Aerodynamic characteristics in pitch of a $35^\circ$ swept wing model with and without a $0.02b/2$ notch at $0.74b/2$ ; horizontal tail on and off; $\delta_f = 50^\circ$ . . . . .	15
Comparison of the effects of a chordwise fence, leading-edge chord-extension, and a $0.02b/2$ notch on aerodynamic characteristics in pitch; $\Lambda = 35^\circ$ . . . . .	16
Effects of horizontal-tail span on aerodynamic characteristics in pitch; $\Lambda = 35^\circ$ . . . . .	17
Effect of wing sweep on aerodynamic characteristics in pitch of a model having swept tail surfaces . . . . .	18

Effect of aspect ratio on the aerodynamic characteristics in pitch of a model having an unswept wing and swept tail surfaces . . . . .	19
Effect of horizontal-tail position on aerodynamic character- istics in pitch of an unswept-wing model of aspect ratio 2.50 . .	20
Surface tuft photographs for the $35^{\circ}$ swept-wing model with or without a $0.02b/2$ notch at $0.74b/2$ ; $\delta_f = 0^{\circ}$ . . . . .	21

### Effect of Various Leading- and Trailing-Edge Devices

#### and Horizontal-Tail Span on the Swept-Wing Model

The following discussion is concerned with the results of tests made to determine the effects of various leading-edge flow-control notches and leading- and trailing-edge modifications on the longitudinal instability (pitch-up) of the  $35^{\circ}$  swept-wing model employed in this investigation. In order to facilitate the discussion only the angle-of-attack range where the original model, configuration 1, was unstable ( $\alpha = 8^{\circ}$  to  $\alpha = 16^{\circ}$ ) is being considered, unless otherwise noted.

The data of figure 8(a) indicate that a  $0.02b/2$  notch located inboard of  $0.60b/2$  (configurations 2 and 3) has little effect on the longitudinal stability of the model. With the notch at  $0.60b/2$  (configuration 4) the model is about neutrally stable although short-lived pitch-ups do occur at higher angles of attack. An outboard movement of the notch from  $0.6b/2$  to  $0.74b/2$  (configuration 12) has little additional beneficial effect on the stability for angles of attack up to about  $20^{\circ}$ , above which the effects of notch movement are generally erratic.

The  $0.02b/2$  notch at  $0.74b/2$  (configuration 12) was selected as the optimum since this arrangement had neutral stability from about  $\alpha = 10^{\circ}$  to  $\alpha = 15^{\circ}$  and a pitch-up did not occur until  $\alpha = 23^{\circ}$  was reached. In addition, a further outboard movement of the notch (configurations 13, 14, and 15) resulted in longitudinal instability occurring at about  $\alpha = 11^{\circ}$  (fig. 8(b)) and the various modifications to the  $0.02b/2$  notch, including reducing the span to  $0.01b/2$ , were detrimental (figs. 9 and 10).

The lift coefficient is increased by as much as 0.1 for angles of attack above  $12^{\circ}$  depending on the spanwise position of the notch (fig. 8(b)). The notches have essentially no effect on the drag coefficient of the model (fig. 8(c)).

Since the separation vortex, which caused a rapid increase in the rate of change of downwash angle with angle of attack at the horizontal tail, emanates near the wing-fuselage juncture (ref. 2), various spans

of notches with the inboard edge at the wing-fuselage juncture were tested (in combination with the 0.02b/2 notch at 0.74b/2) in order to determine their effect on the stability of the model. The wing-fuselage juncture notches (fig. 11) generally are unsatisfactory since they result in slight instability at about an angle of attack of 12°. Before the instability occurs these notches, however, increase the stability of the model. None of the combinations result in better stability than the 0.02b/2 notch at 0.74b/2 (configuration 12).

Various leading- and trailing-edge extensions were investigated in combination with the 0.02b/2 notch at 0.074b/2 and, in general, none of these combinations were satisfactory (figs. 12 and 13). It is interesting to note that the use of a 0.02b/2 notch on a 0.10b/2 airfoil-shaped leading-edge chord-extension having the inboard end at 0.68b/2 (configuration 41) decreased the effectiveness of the extension such that the slight model stability was reduced to instability (fig. 13).

A comparison of the aerodynamic characteristics in pitch of the model with and without the 0.02b/2 notch at 0.74b/2 with the horizontal tail on and off for plain flaps neutral and deflected 50° is presented in figures 14 and 15. The tail-on data with  $\delta_f = 0$  for the original swept-wing are replotted in figure 14 for ease of comparison. The notch generally has little effect on the stability of the model with the tail off ( $\delta_f = 0^\circ$  or  $50^\circ$ ) but, with the tail on, it provides about neutral stability where the pitch-up occurs for the original model ( $\delta_f = 0^\circ$  or  $50^\circ$ ) (figs. 14 and 15).

A comparison of the effects of a chordwise fence, a leading-edge chord-extension, and a 0.02b/2 notch at 0.74b/2 (fig. 16) on the stability of the model indicates that the chord-extension generally is more satisfactory since the region of neutral stability is the smallest for this arrangement. The fence and notch arrangements generally have about the same stability characteristics (the spanwise location was about the same for these two different devices). The surface tuft photographs (fig. 21) indicate that the notch improved the flow over the outer portion of the wing for angles of attack greater than 0° as did the fence and chord-extension (ref. 2).

The effects of horizontal-tail span on the aerodynamic characteristics in pitch of the model (fig. 17) were determined by cutting portions from the tips of the tail so that the area as well as the span was reduced. Decreasing the horizontal-tail span decreased the stability at  $\alpha = 0^\circ$  and slightly improved the stability at about  $\alpha = 11^\circ$  ( $C_L$  about 0.8). This improvement does not appear to be sufficient to overcome the pitch-up if the static margin at  $C_L = 0$  for the shortest span arrangement is increased to the original static margin because at higher lift coefficients the instability with the shortest tail span (about 70 percent original span) is greater than with the original tail span.

Longitudinal Stability Characteristics  
of Model with Unswept Wing

It has been shown by means of the tuft grid technique (ref. 9) that the tip vortex on an unswept wing remains at or very near the wing tip as the angle of attack is increased. Thus, by cutting portions from the tips of an unswept wing to reduce the aspect ratio it is possible to have a controlled inboard movement of the tip vortex. If the horizontal-tail span is constant for all aspect ratios, the wing tip vortex approaches the tip of the tail and, if the aspect ratio is reduced sufficiently, passes inboard of the tip of the horizontal tail. The following discussion covers the results of a series of tests made to study the effect of vortex span on the longitudinal stability characteristics of a model having swept tail surfaces.

The effect of decreasing the wing sweep (0.333 chord line) from  $35^\circ$  to  $0^\circ$  on the aerodynamic characteristics in pitch is shown in figure 18. The unswept-wing model, although not able to reach as high a lift coefficient as the swept-wing model, has a greater useful range of lift coefficient since the swept-wing model encounters a pitch-up at about  $\alpha = 10^\circ$ . The unswept-wing model has a slight pitch-up at about  $\alpha = 19^\circ$  but this is above  $C_L_{max}$ .

A reduction in aspect ratio (and vortex span) from 3.57 to 2.50 generally has little effect on the longitudinal stability of the model (fig. 19(a)). With a further reduction in aspect ratio to 2.25 a pitch-up occurs at about  $C_L = 0.4$ ; a further decrease in aspect ratio results in a more severe pitch-up. In the low-lift-coefficient range ( $C_L$  less than 0.3) a reduction in aspect ratio from 2.25 to 1.00 results in a large increase in stability, the most severe pitch-up occurring at high lift coefficients. For a given angle of attack a reduction in aspect ratio decreases the lift coefficient for angles of attack up to about  $18^\circ$  (fig. 19(a)) and for a given lift coefficient a decrease in aspect ratio results in an increase in the drag coefficient (fig. 19(b)).

It was indicated in the investigation of reference 5 that for a  $35^\circ$  swept-wing model lowering the horizontal tail resulted in better over-all longitudinal stability characteristics. The same tail positions and tail were investigated in the present investigation with the aspect ratio 2.50 unswept wing (fig. 20). For the unswept-wing model the high tail position appears to be above the wake of the wing and static longitudinal stability exists for the entire lift-coefficient range investigated. Lowering the tail, and also slightly decreasing the tail length, results in instability at the lowest lift coefficient investigated (fig. 20). The tail evidently moves into the wake as it is lowered and with the tail on the fuselage center line it is still in the wake because of the wing incidence.

The investigation of reference 10 using a similar model with an aspect ratio 2.50 unswept wing indicated trends similar to those obtained in the present investigation for tail positions above the wing-chord plane.

### CONCLUSIONS

An investigation conducted in the Langley stability tunnel to determine the effects of various leading-edge flow-control notches and associated devices, horizontal-tail span, wing sweep, aspect ratio of an unswept wing, and horizontal-tail position on the longitudinal stability characteristics of an airplane model have indicated the following conclusions:

1. Of the single leading-edge flow-control notches investigated a 2 percent semispan notch at 74 percent semispan from the plane of symmetry had the best over-all stability characteristics, although the notch did not provide better than neutral stability where the original  $35^{\circ}$  swept-wing model was unstable (plain flaps neutral or deflected). Various changes in this notch, including reducing the span, had a detrimental effect on the effectiveness of the notch in reducing the pitch-up.
2. A comparison of the effects of a chordwise fence, a chord-extension and the best notch on the longitudinal stability of the  $35^{\circ}$  swept-wing model indicated the chord-extension to be the most favorable device since the region of neutral stability was the smallest. The fence and notch arrangements had about the same longitudinal stability characteristics.
3. Reducing the horizontal-tail span to about 70 percent of its original span did not result in satisfactory stability for the plain swept-wing model.
4. Decreasing the sweep of the wing from  $35^{\circ}$  to  $0^{\circ}$  had a beneficial effect on the stability of the model since the unswept wing was longitudinally stable for lift coefficients through maximum whereas a pitch-up occurred for the swept wing at about a lift coefficient of 0.8.
5. A decrease in aspect ratio (and vortex span) of the unswept wing from 3.57 to 2.50 had little effect on the longitudinal stability of the model. However, a further reduction in aspect ratio resulted in a pitch-up at a low lift coefficient which became more severe as the aspect ratio was decreased to 1.00.

6. For the aspect ratio 2.50 unswept-wing model, lowering the horizontal tail had a detrimental effect on the stability of the model at low angles of attack since the tail apparently moved into the wing wake.

Langley Aeronautical Laboratory,  
National Advisory Committee for Aeronautics,  
Langley Field, Va., August 21, 1953.

## REFERENCES

1. Queijo, M. J. and Jaquet, Byron M.: Wind-Tunnel Investigation of the Effect of Chordwise Fences on Longitudinal Stability Characteristics of an Airplane Model With a  $35^{\circ}$  Sweptback Wing. NACA RM L50K07, 1950.
2. Jaquet, Byron M.: Effect of Chord Discontinuities and Chordwise Fences on Low-Speed Static Longitudinal Stability of an Airplane Model Having a  $35^{\circ}$  Sweptback Wing. NACA RM L52C25, 1952.
3. Jaquet, Byron M.: Effects of Chord-Extension and Droop of Combined Leading-Edge Flap and Chord-Extension on Low-Speed Static Longitudinal Stability Characteristics of an Airplane Model Having a  $35^{\circ}$  Sweptback Wing With Plain Flaps Neutral or Deflected. NACA RM L52K21a, 1953.
4. Fischel, Jack, and Nugent, Jack: Flight Determination of the Longitudinal Stability in Accelerated Maneuvers at Transonic Speeds for the Douglas D-558-II Research Airplane Including the Effects of an Outboard Wing Fence. NACA RM L53A16, 1953.
5. Campbell, George S., and Weil, Joseph: The Interpretation of Nonlinear Pitching Moments in Relation to the Pitch-Up Problem. NACA RM L53I02, 1953.
6. Queijo, M. J., and Wolhart, Walter D.: Wind-Tunnel Investigation of the Effects of Horizontal-Tail Position on the Low-Speed Longitudinal Stability Characteristics of an Airplane Model With a  $35^{\circ}$  Sweptback Wing Equipped With Chordwise Fences. NACA RM L51H17, 1951.
7. Herriot, John G.: Blockage Corrections for Three-Dimensional-Flow Closed-Throat Wind Tunnels, With Consideration of the Effect of Compressibility. NACA Rep. 995, 1950. (Supersedes NACA RM A7B28.)
8. Gillis, Clarence L., Polhamus, Edward C., and Gray, Joseph L., Jr.: Charts for Determining Jet-Boundary Corrections for Complete Models in 7- by 10-Foot Closed Rectangular Wind Tunnels. NACA WR L-123, 1945 (Formerly NACA ARR L5G31).
9. Bird, John D., and Riley, Donald R.: Some Experiments on Visualization of Flow Fields Behind Low-Aspect-Ratio Wings by Means of a Tuft Grid. NACA TN 2674, 1952.
10. Foster, Gerald V., Mollenberg, Ernst F., and Woods, Robert L.: Low-Speed Longitudinal Characteristics of an Unswept Hexagonal Wing With and Without a Fuselage and a Horizontal Tail Located at Various Positions at Reynolds Numbers From  $2.8 \times 10^6$  to  $7.6 \times 10^6$ . NACA RM L52L11b, 1953.

C [REDACTED] AL

Table I.—Details of leading-edge flow-control notches

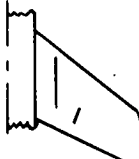
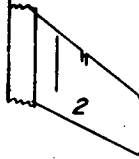
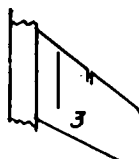
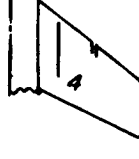
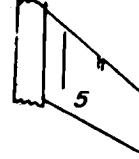
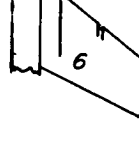
NO.	Plan view	Notch span % b/2	Inboard edge location % b/2	Notch depth % c̄	Type of notch
1		0	—	—	—
2		2	55	5	Both sides parallel to center line
3		2	58	5	
4		2	60	5	
5		2	62	5	
6		2	64	5	

Table I.- Continued

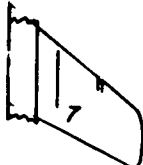
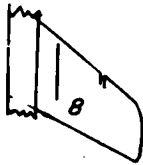
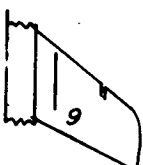
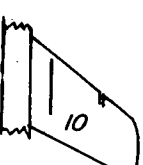
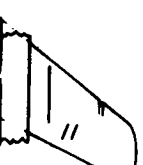
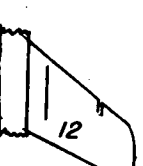
NO.	Plan view	Notch span % b/2	Inboard edge location % b/2	Notch depth % c	Type of notch
7		2	66	5	Both sides parallel to center line
8		2	68	5	
9		2	70	5	
10		2	72	5	
11		2	73	5	
12		2	74	5	

Table I.- Continued

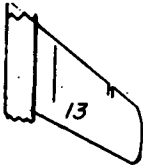
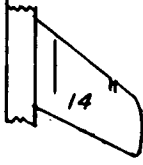
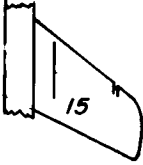
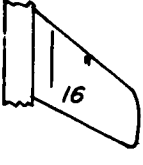
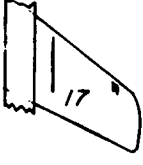
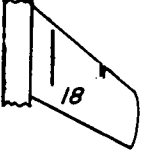
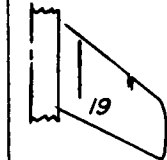
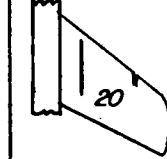
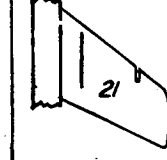
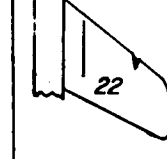
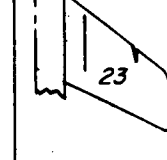
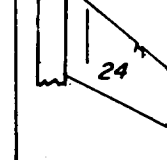
NO.	Plan view	Notch span % b/2	Inboard edge location % b/2	Notch depth % c	Type of notch
13		2	76	5	Both sides parallel to center line
14		2	78	5	
15		2	80	5	
16		2	60	$2\frac{1}{2}$	Both sides parallel to center line. Cap covering notch from 0c to $2\frac{1}{2}c$
17		2	80	$2\frac{1}{2}$	
18		1	72	5	Both sides parallel to center line

Table I.- Continued

NO	Plan view	Notch span % b/2	Inboard edge location % b/2	Notch depth % $\bar{c}$	Type of notch
19		1	73	5	Both sides parallel to center line
20		1	74	5	
21		1	76	5	
22		2	73	5	V notch
23		1	73	5	V notch
24		2 at leading- edge 4 at 15% $\bar{c}$	74	5	Flared notch

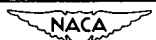


Table I.- Continued

NO.	Plan view	Notch span % b/2	Inboard edge location % b/2	Notch depth % C	Type of notch
25		2	74	5	Skewed
26		2	60 and 74	5	Multiple notches parallel to center line
27		2	Wing-fuselage juncture	5	Both sides parallel to center line
		2	74	5	
28		4	Wing-fuselage juncture	5	
		2	74	5	
29		8	Wing-fuselage juncture	5	
		2	74	5	
30		12	Wing-fuselage juncture	5	
		2	74	5	

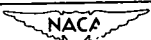


Table I- Continued

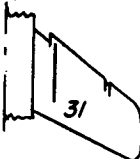
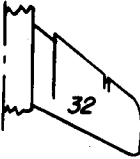
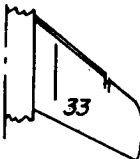
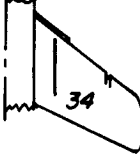
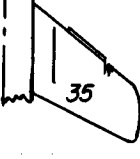
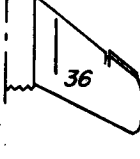
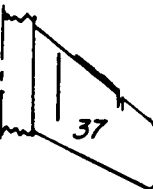
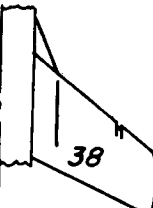
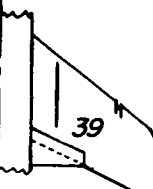
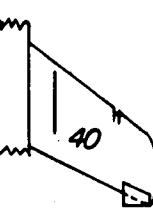
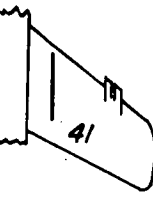
NO.	Plan view	Notch span % b/2	Inboard edge location % b/2	Notch depth % c	Type of notch
31		12	Wing-fuselage juncture	10	Both sides parallel to center line
		2	74	5	
32		15	Wing fuselage juncture	10	
		2	74	5	
33		2	74	5	
34		2	74	5	
35		2	74	5	
36		2	74	5	



Table I - Concluded

NO.	Plan view	Notch span % b/2	Inboard edge location % b/2	Notch depth % C	Type of notch
37		2	74	5	Both sides parallel to center line
38		2	74	5	
39		2	74	5	
40		2	74	5	
41		2	74	5	

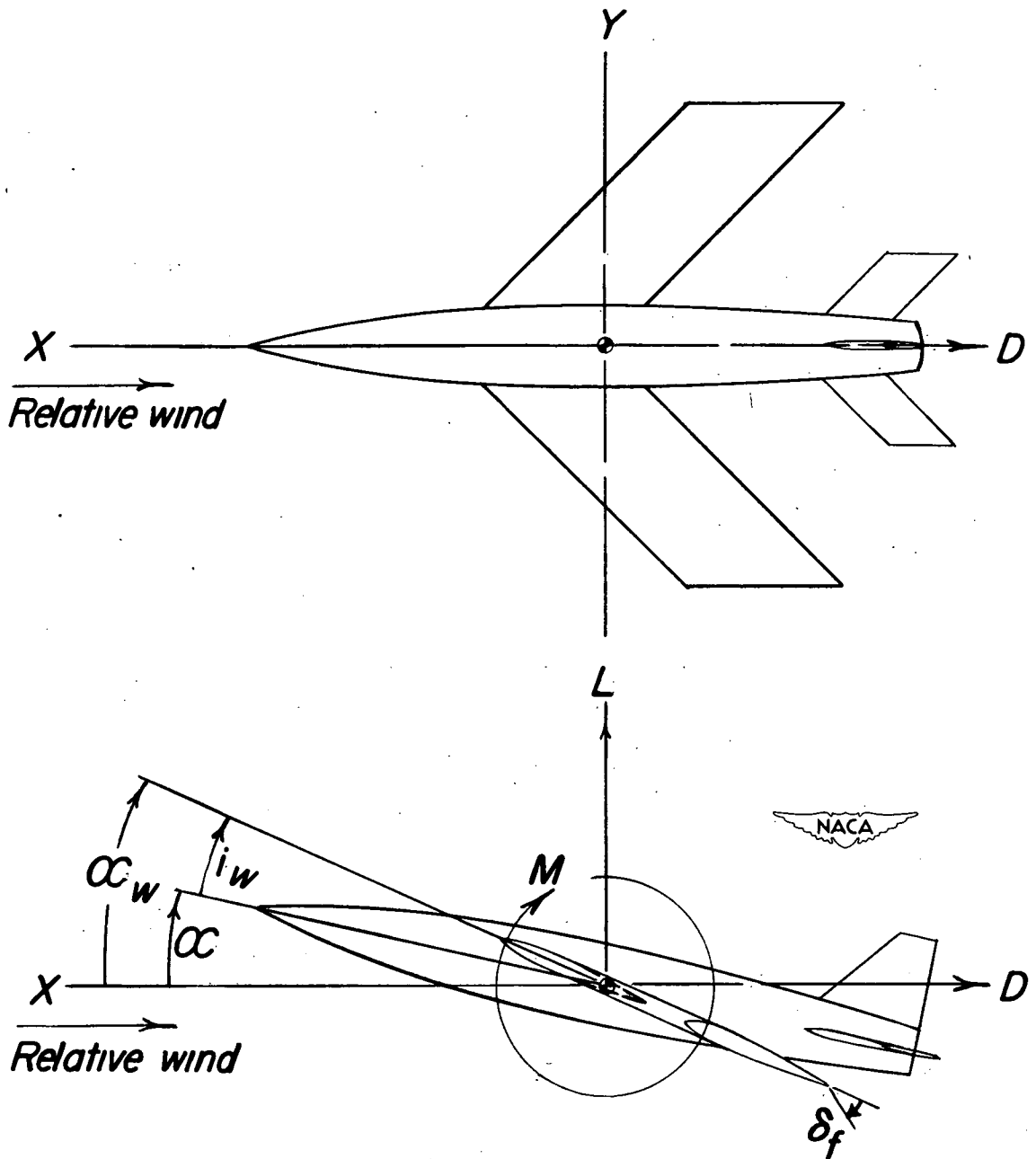


Figure 1.- Stability system of axes. Arrows indicate positive direction of forces, moments, and angular displacements.

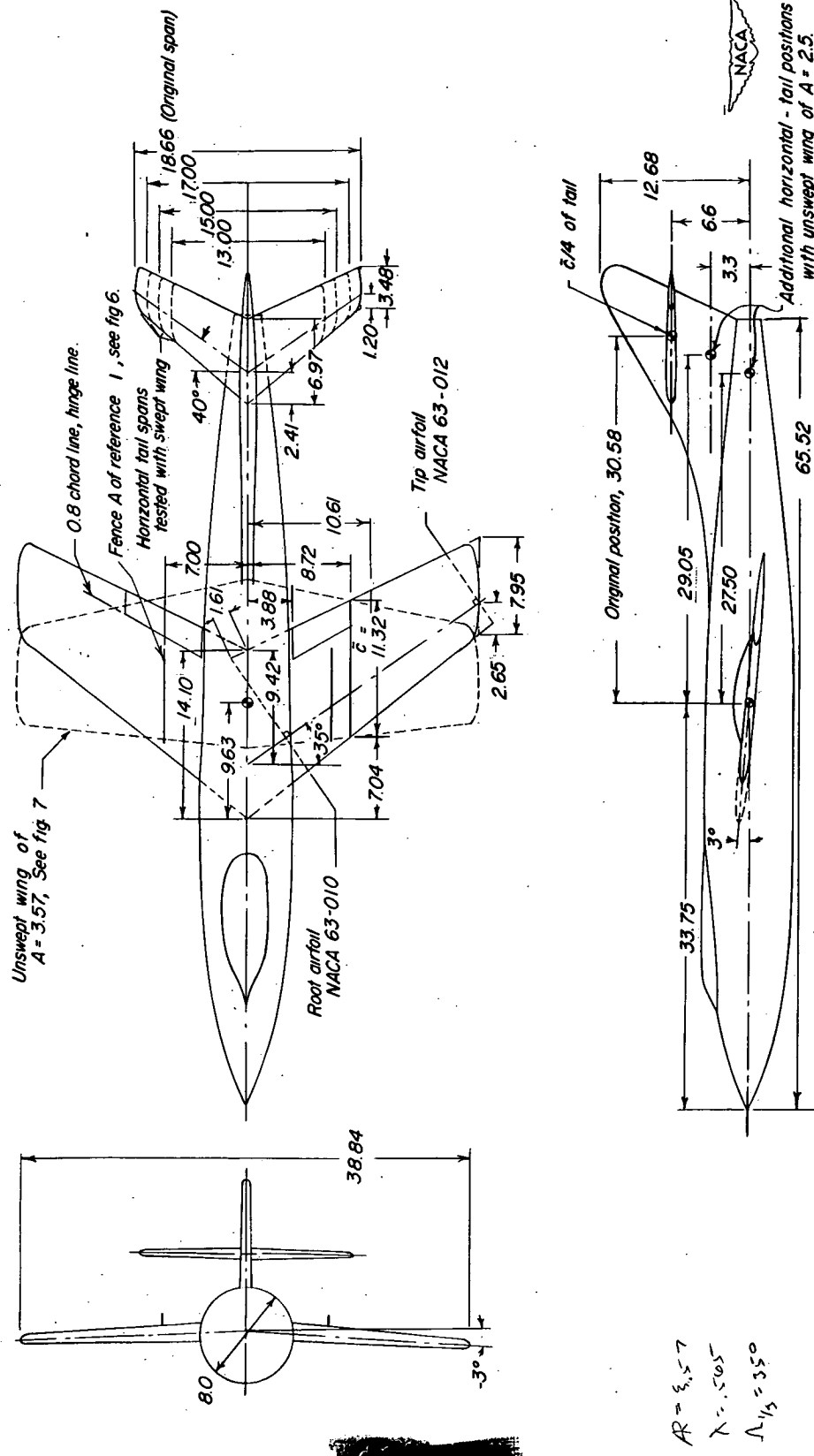
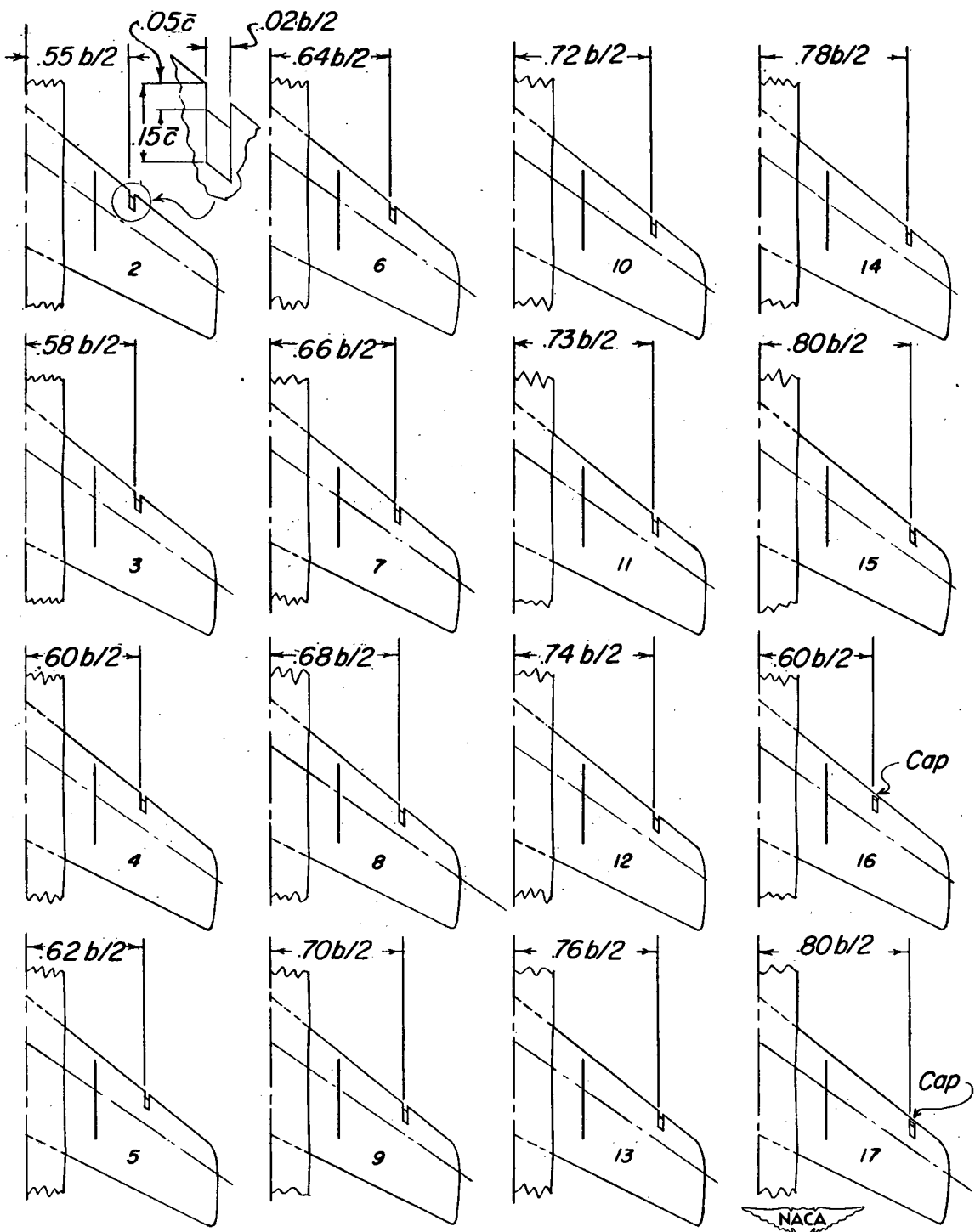
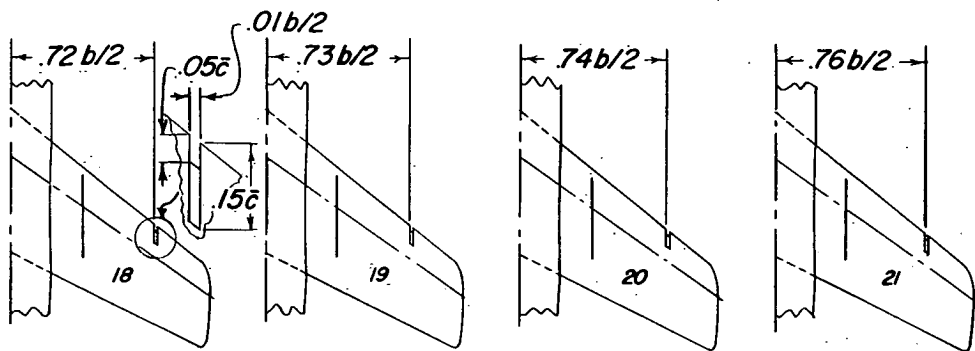
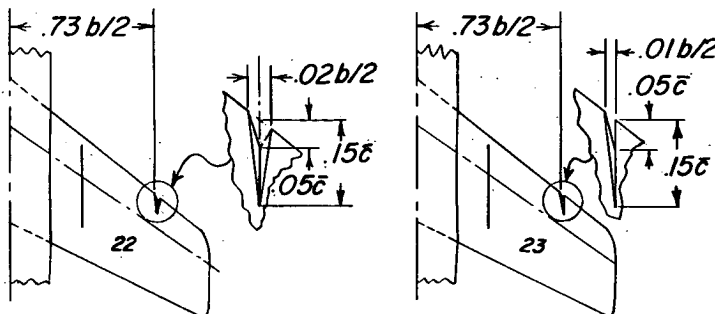


Figure 2.- Geometry of model. All dimensions are in inches.

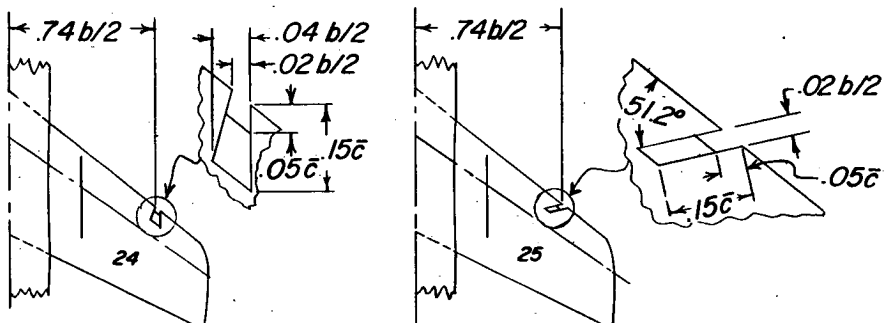
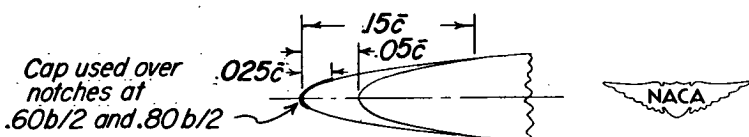


(a) 0.02b/2 notches with both faces parallel to airstream.

Figure 3.- Detail and locations of single notches.

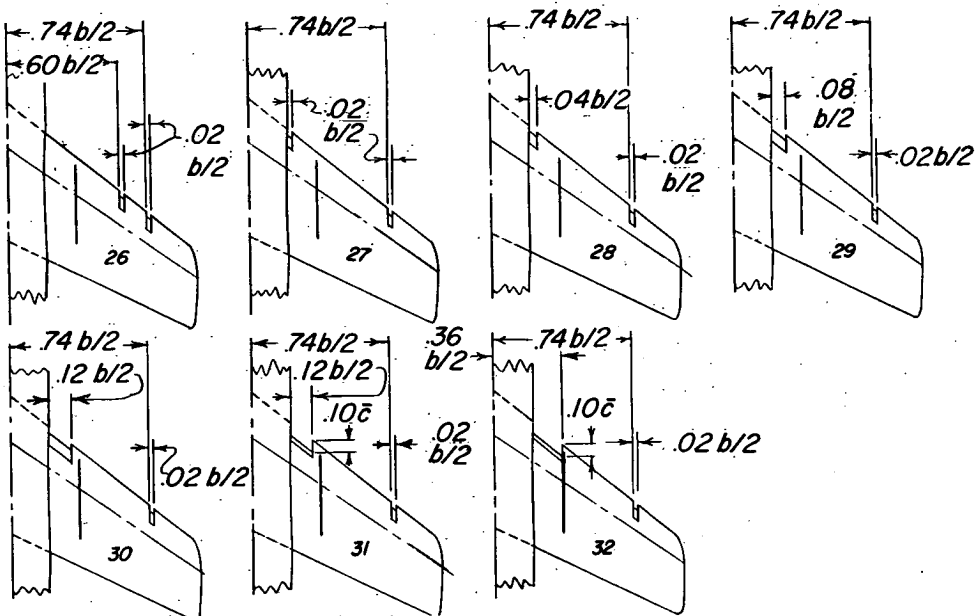
(b)  $0.01b/2$  notches with both faces parallel to airstream.

(c) V-notches.

(d) Variations of  $0.02b/2$  notch.

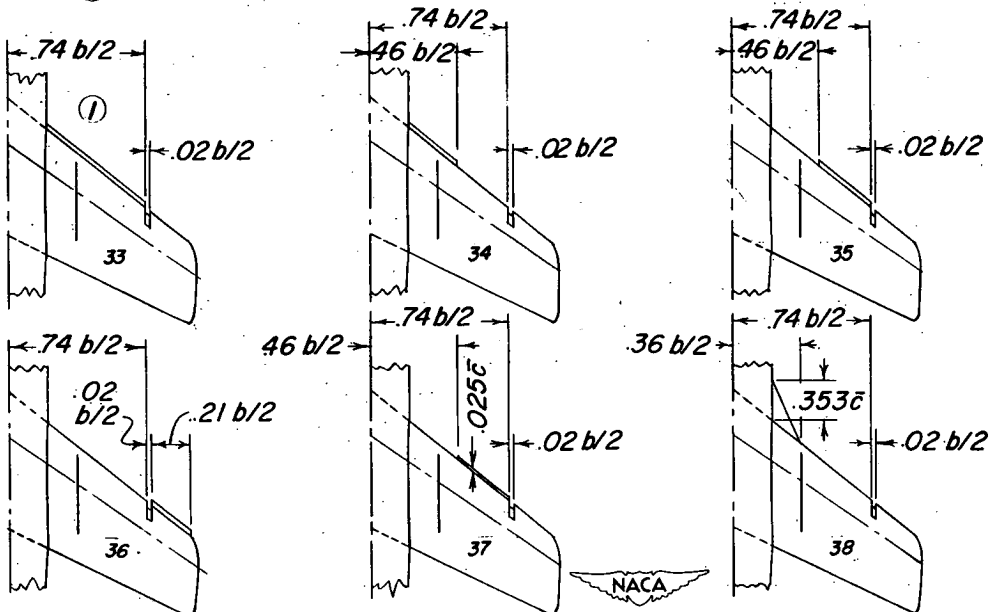
(e) Typical profile through notch.

Figure 3.- Concluded.



(a) Multiple notches. Streamwise depth of notches is  $0.05\bar{c}$  unless otherwise noted.

① Also tested without notch at  $.74b/2$ .



(b) Notch and sharp-leading edge combinations. Streamwise depth of extensions is  $0.05\bar{c}$  unless otherwise noted. Thickness of extensions,  $0.08\bar{c}$ .

Figure 4.- Details of multiple notches and combinations of sharp-leading edge extensions with a  $0.02b/2$  notch at  $0.74b/2$ .

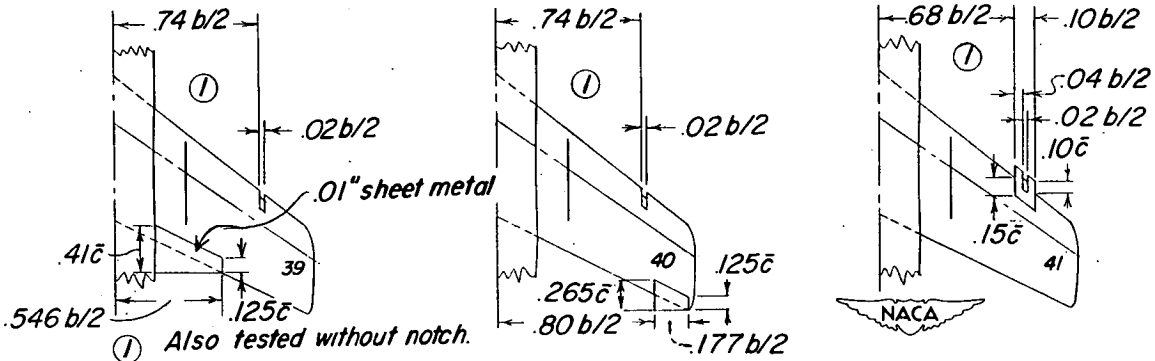
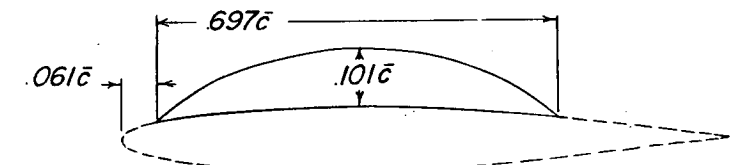
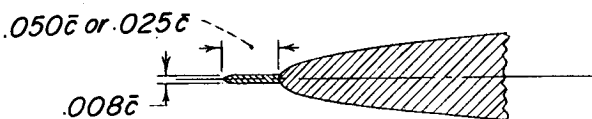


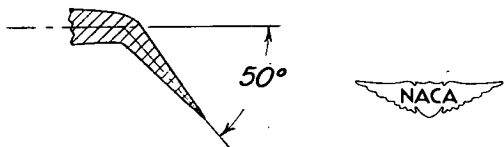
Figure 5.- Trailing-edge extensions and airfoil-shaped leading-edge extension in combination with a  $0.02b/2$  notch.



*Profile of fence A of reference 1 and chordwise location for present tests.*

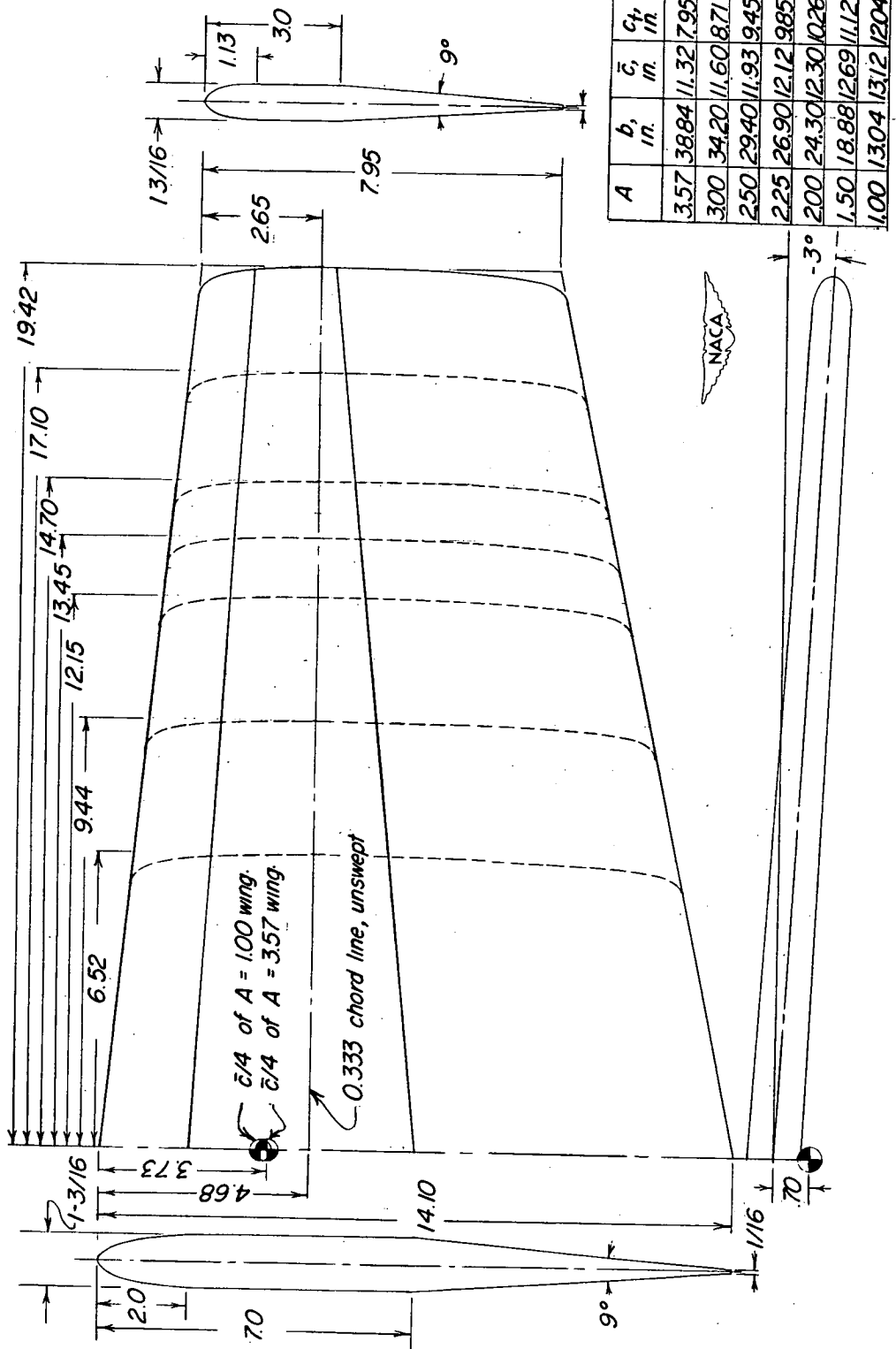


*Typical section through sharp leading-edge extension*



*Typical section through flap normal to hinge line*

Figure 6.- Details of fence A, section through sharp leading-edge extension, and section through trailing-edge flap.



$A$	$b_1$ in.	$\bar{c}_1$ in.	$c_t$ in.	$S_1$ sq.in.	$1$
3.57	38.84	11.32	7.95	428	.565
300	34.20	11.60	8.71	390	617
250	29.40	11.93	9.45	346	670
225	26.90	12.12	9.85	322	698
200	24.30	12.30	10.26	296	727
150	18.88	12.69	11.12	238	788
100	13.04	13.12	12.04	171	855

Figure 7.- Details of unswept wings investigated. All dimensions are in inches.

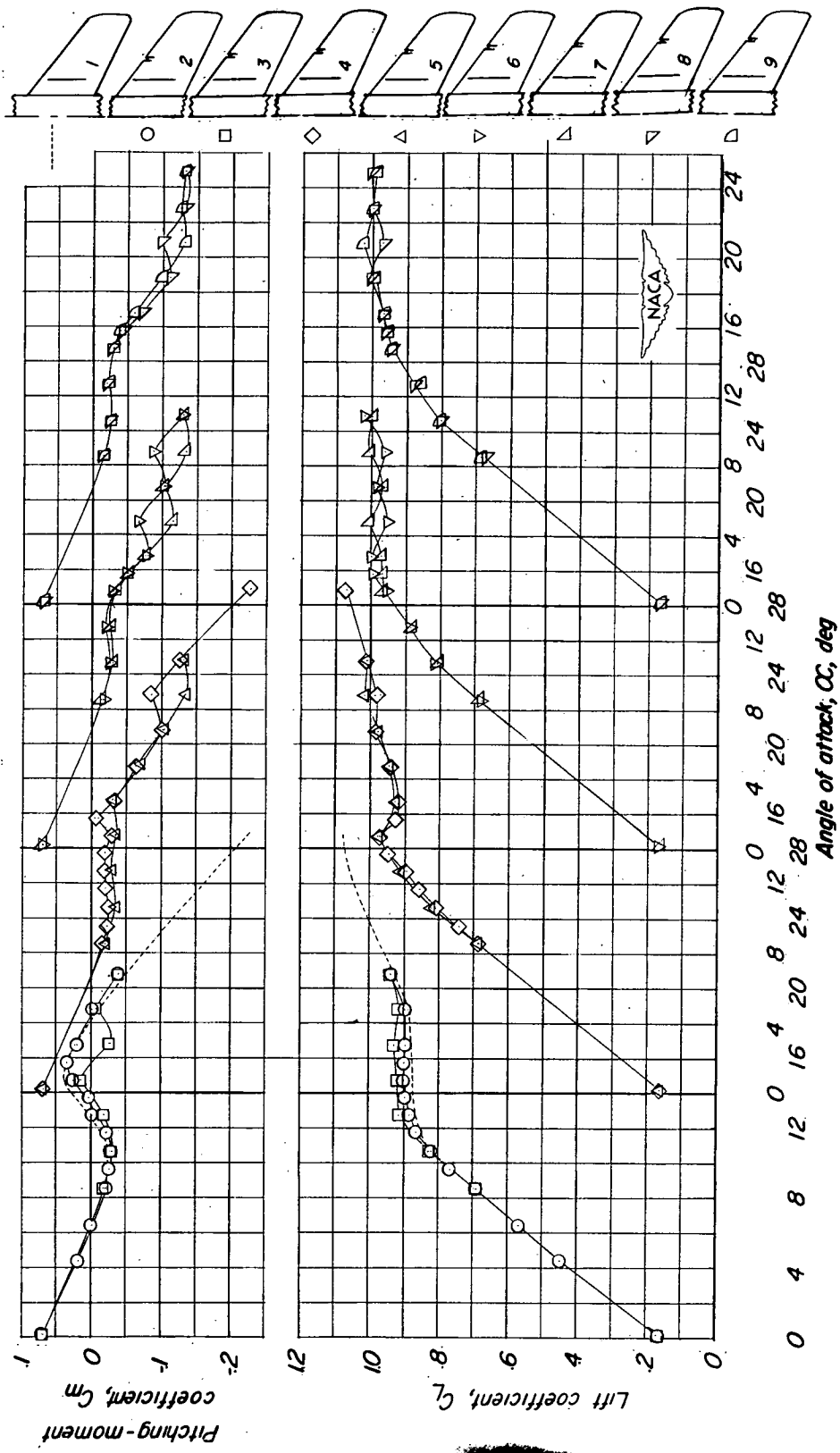
(a) Variation of  $C_m$  and  $C_L$  with  $\alpha$ .

Figure 8.- Effect of spanwise position of 2 percent semispan leading-edge flow-control notches on the aerodynamic characteristics in pitch of a 35° swept-wing model.  $\delta_f = 0^\circ$ .

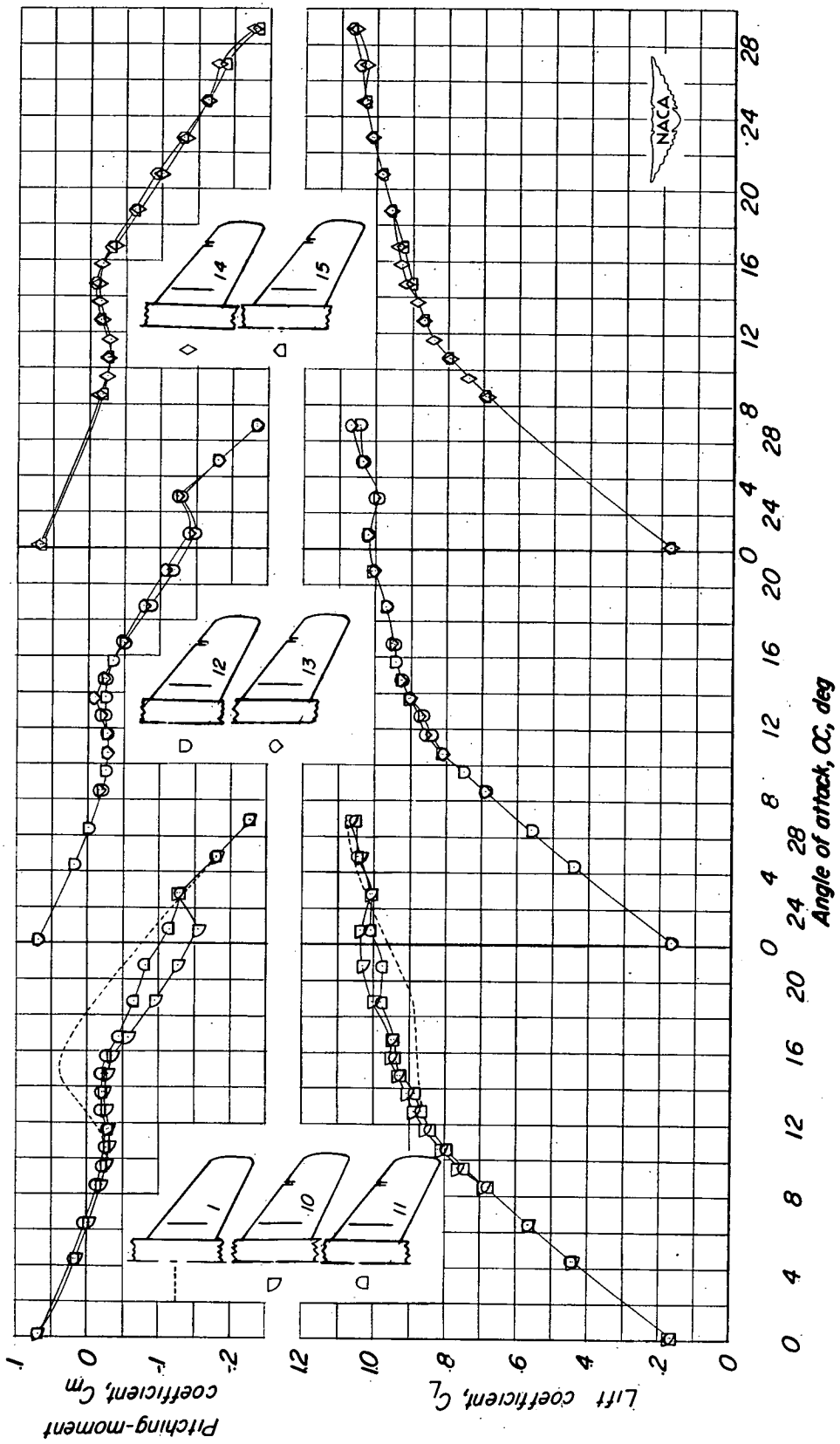
(b) Variation of  $C_m$  and  $C_L$  with  $\alpha$ .

Figure 8.- Continued.

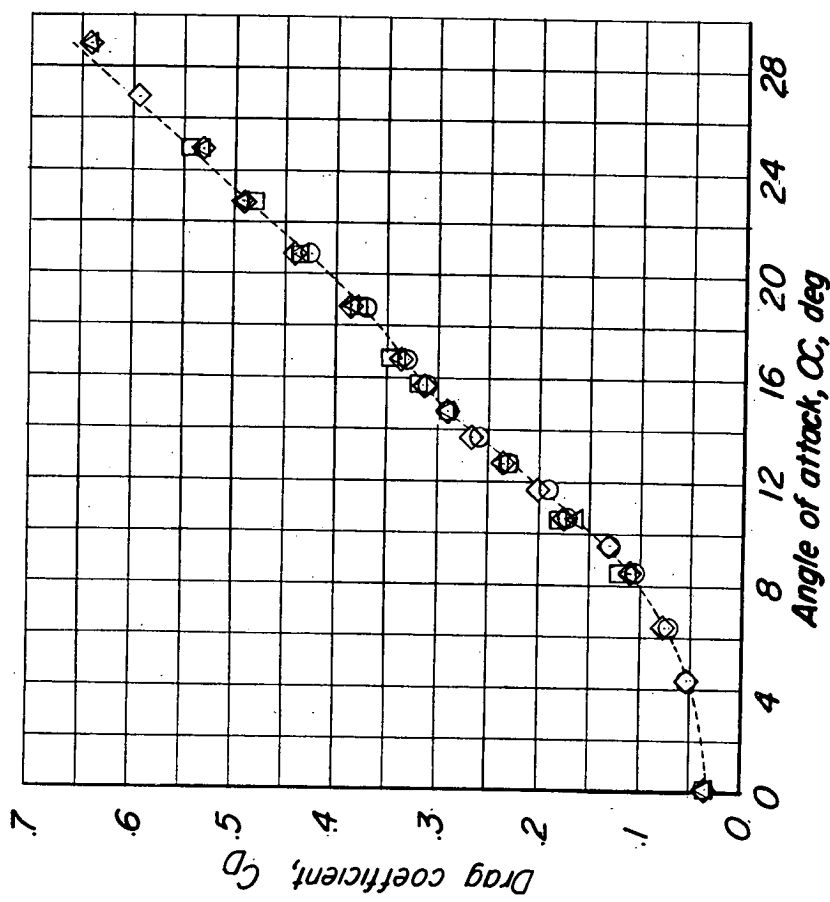
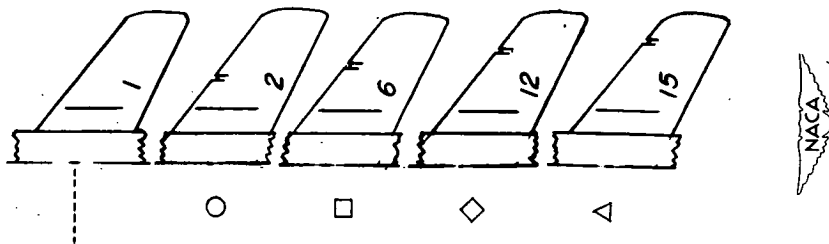
(c) Variation of  $C_D$  with  $\alpha$ .

Figure 8.- Concluded.

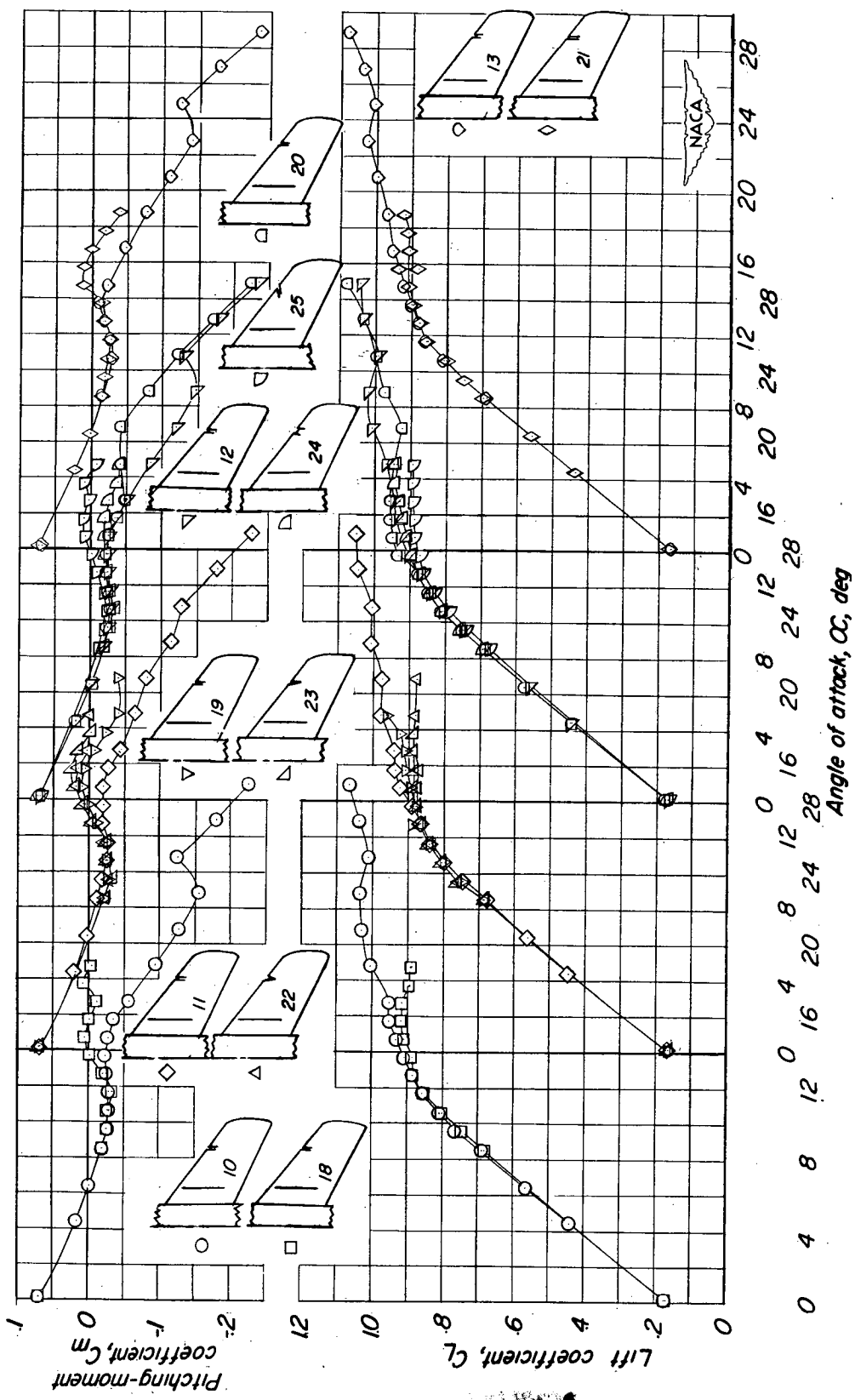


Figure 9.—Effects of span of leading-edge flow-control notches and variations of the notches on aerodynamic characteristics in pitch of a 35° swept-wing model.  $\delta_f = 0^\circ$ .

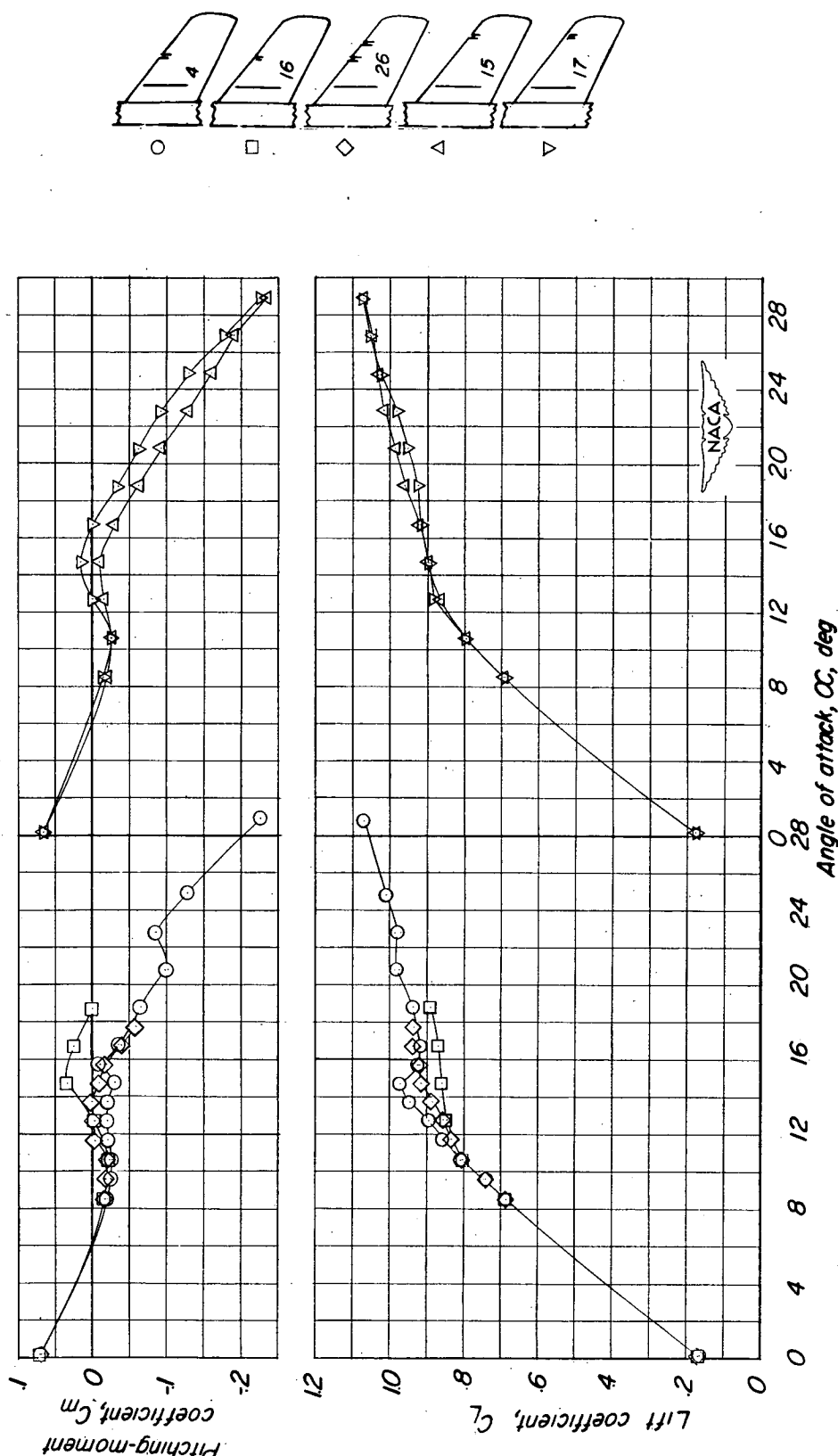


Figure 10.- Effect of closing notch leading-edge and a multiple-notch arrangement on the aerodynamic characteristics in pitch of a 35° swept-wing model.  $\delta_f = 0^\circ$ .

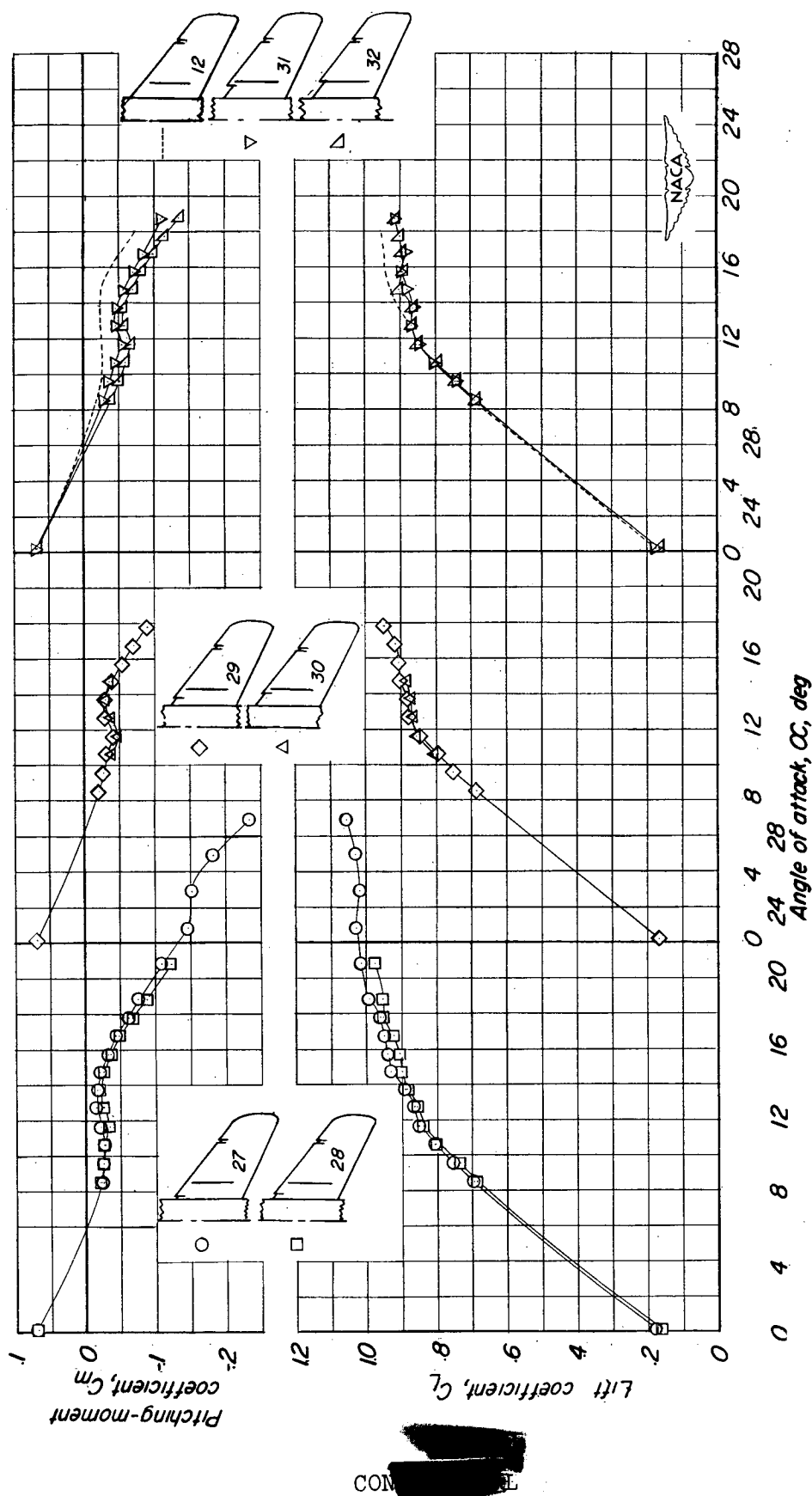


Figure 11.- Effect of span and chord of wing-fuselage juncture notches on aerodynamic characteristics in pitch of a  $35^\circ$  swept-wing model.  
 $\delta_f = 0^\circ$ .

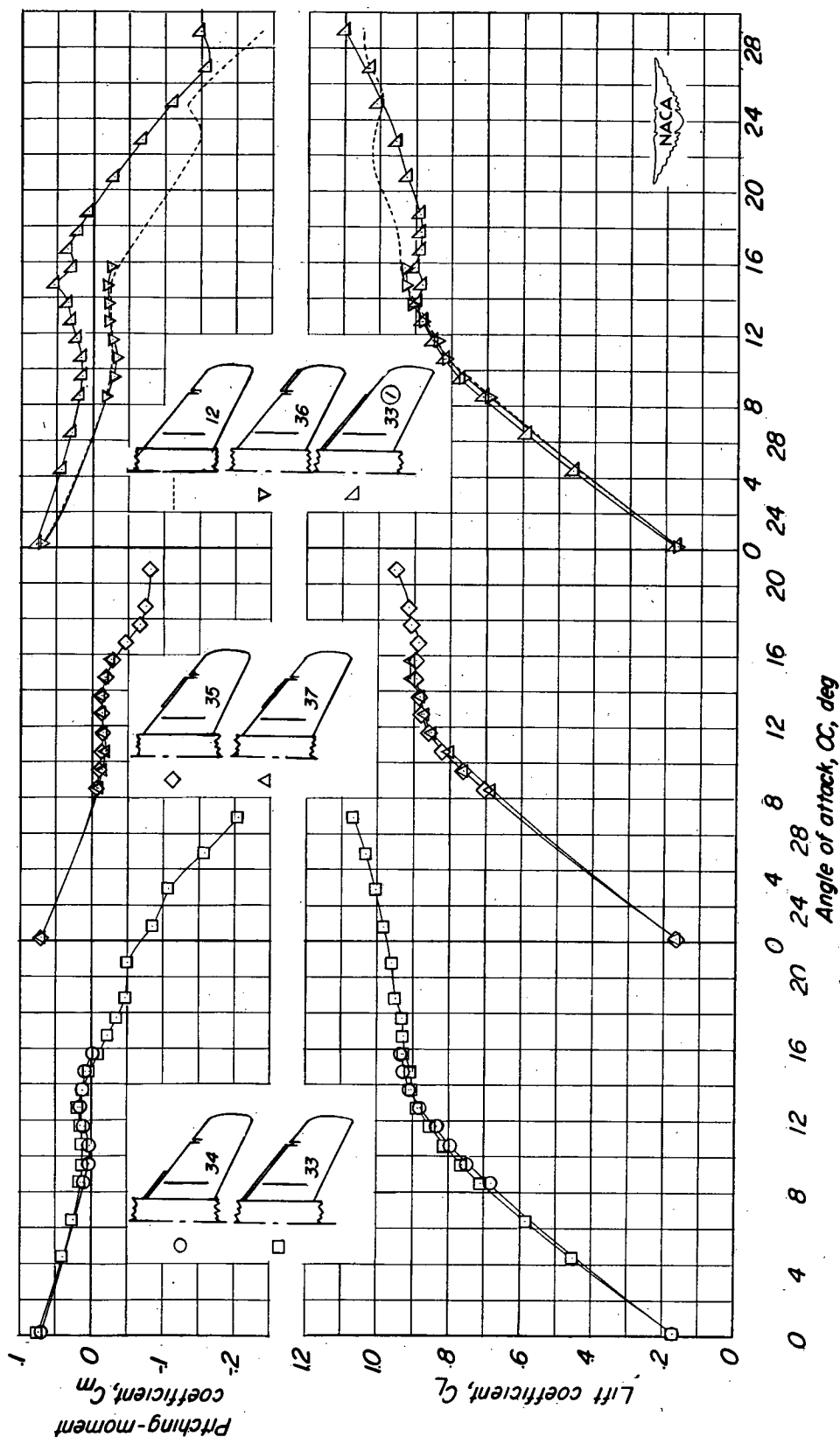


Figure 12.— Effect of sharp leading-edge extensions in combination with a 2 percent semispan leading-edge flow-control notch at 74 percent semispan on aerodynamic characteristics in pitch of a 35° swept-wing model.  $\delta_f = 0^\circ$ .

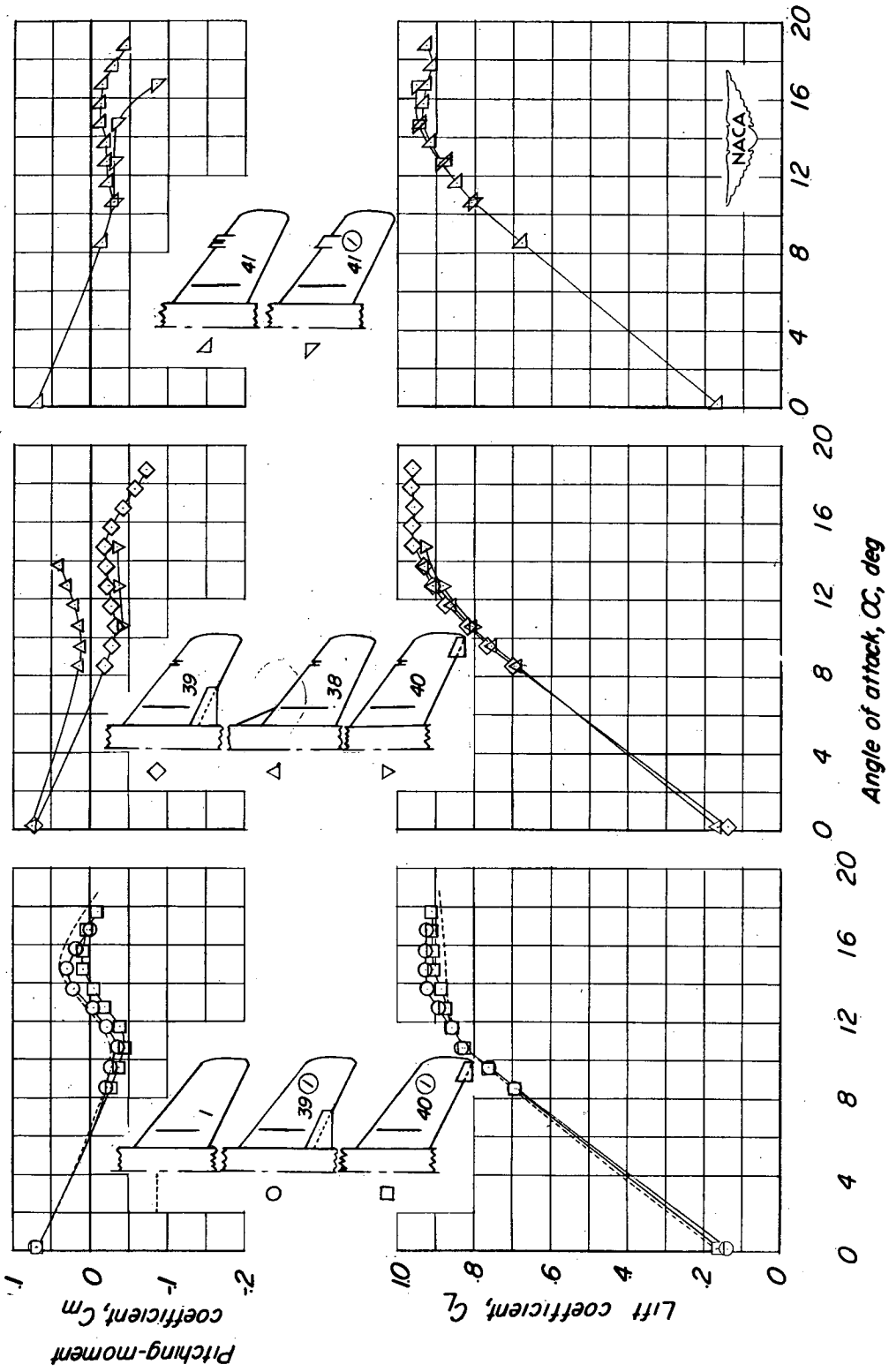


Figure 13.- Effect of various leading- and trailing-edge extensions on the aerodynamic characteristics in pitch of a 35° swept-wing model.  
 $\delta_f = 0^\circ$

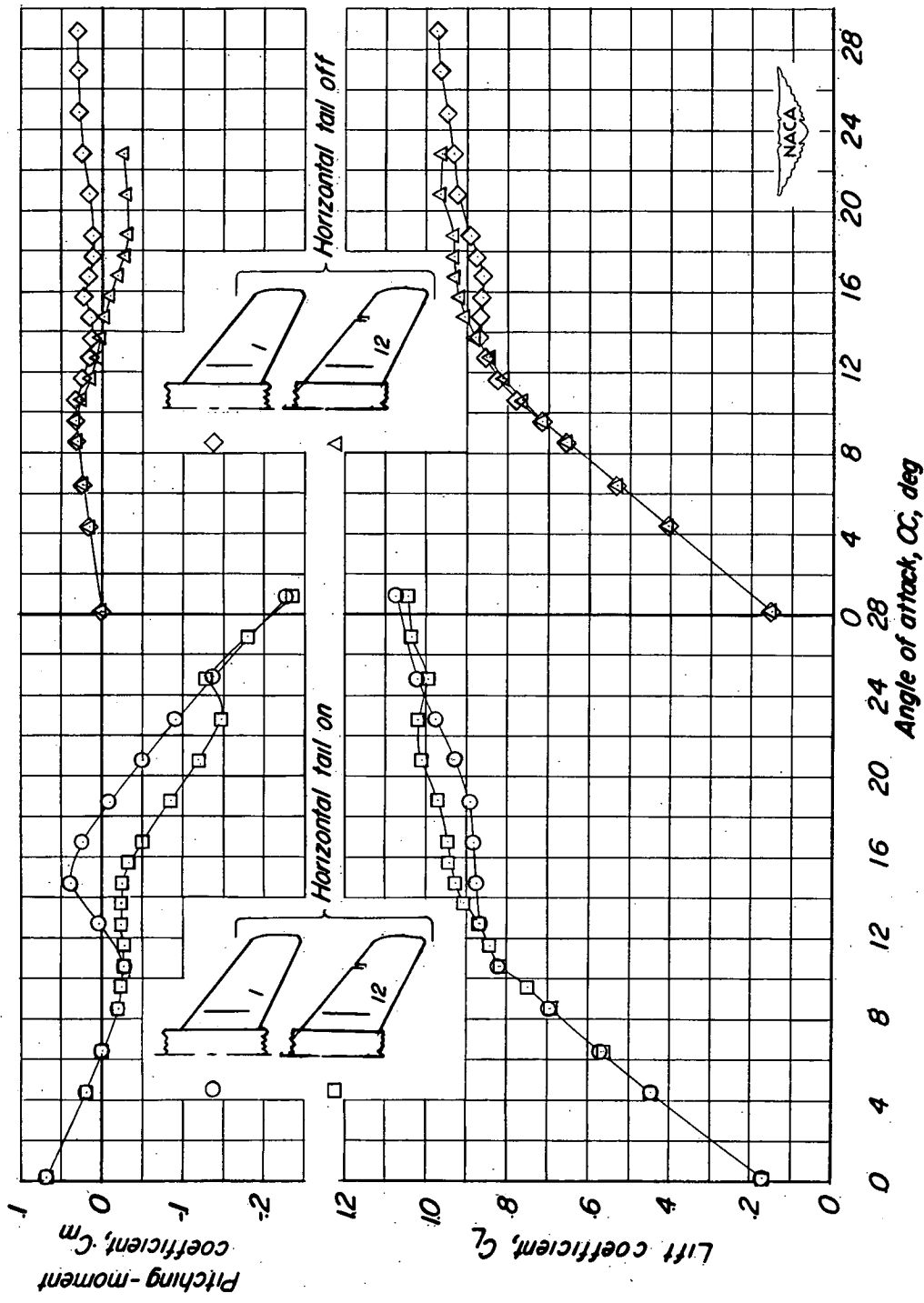


Figure 14.- Aerodynamic characteristics in pitch of a  $35^\circ$  swept-wing model with or without a 2 percent semispan leading-edge flow-control notch at 74 percent semispan. Horizontal tail on and off.  $\delta_f = 0^\circ$ .

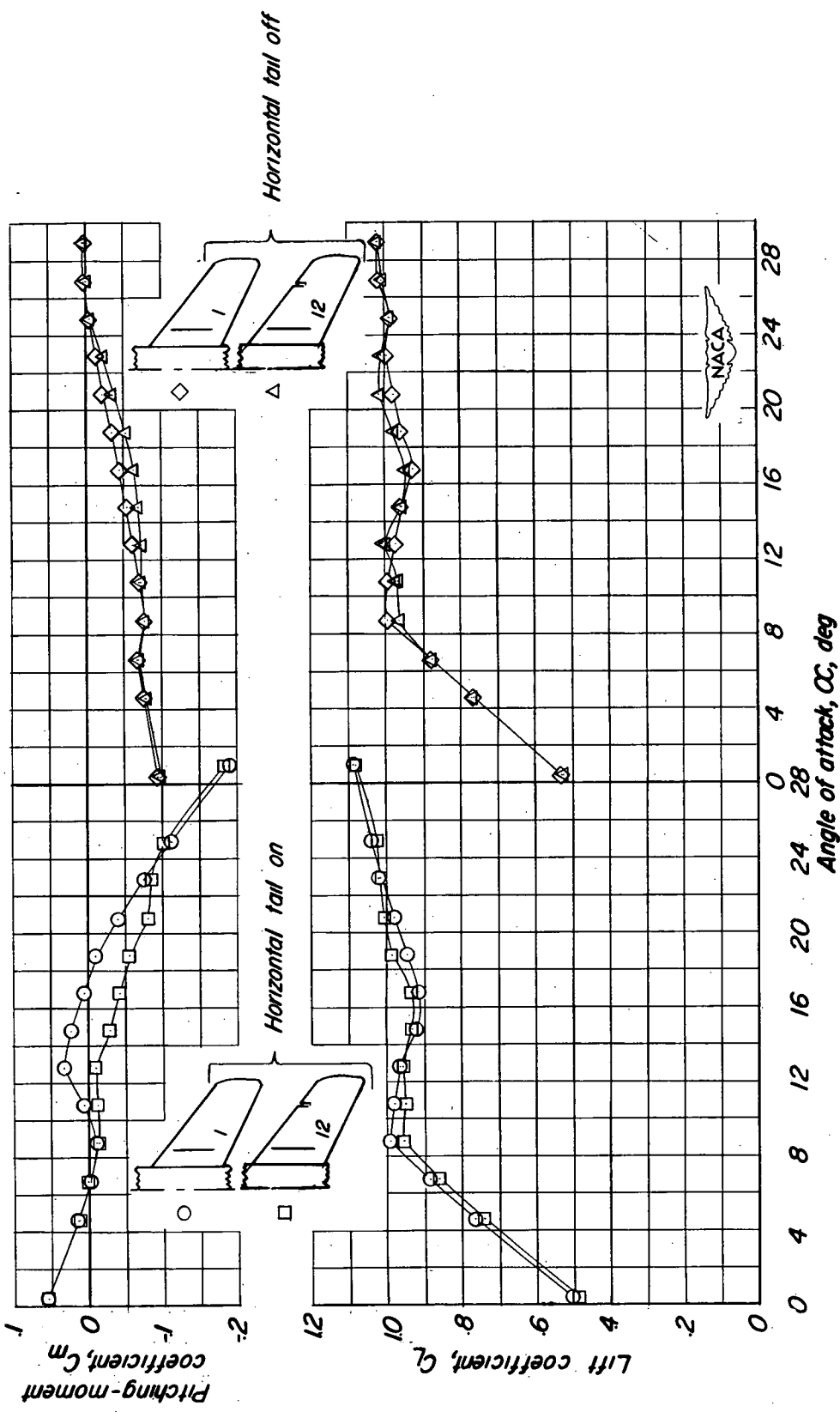


Figure 15.—Aerodynamic characteristics in pitch of a  $35^\circ$  swept-wing model with or without a 2 percent semispan leading-edge flow-control notch at  $7\frac{1}{4}$  percent semispan. Horizontal tail on and off.  $\delta_f = 50^\circ$ . Landing gear and doors off.

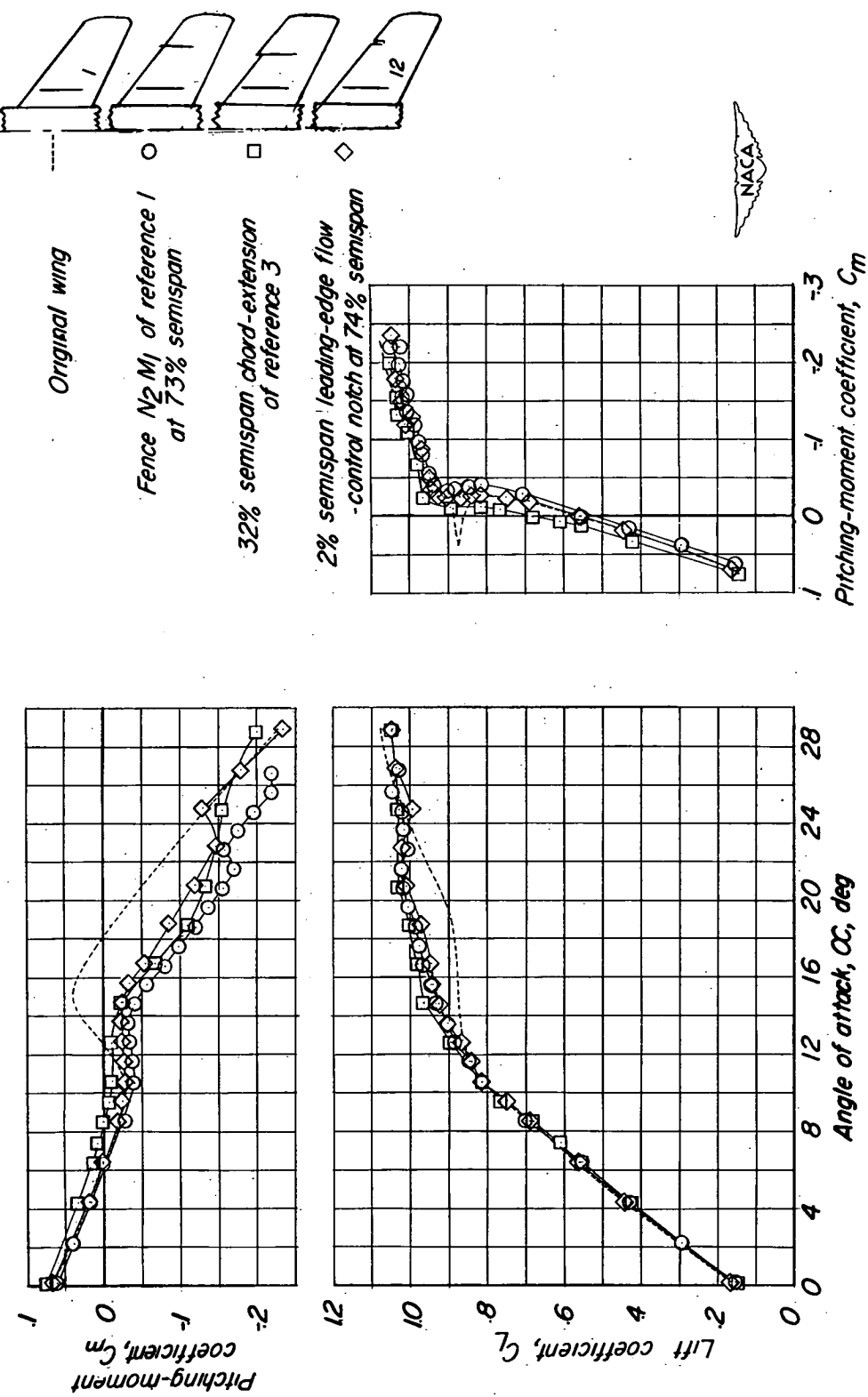


Figure 16.- Comparison of the effects of a chordwise fence, leading-edge chord extension, and a 2 percent semispan leading-edge flow-control notch on the aerodynamic characteristics in pitch of a 350 swept-wing model.  $\delta_f = 0^\circ$ .

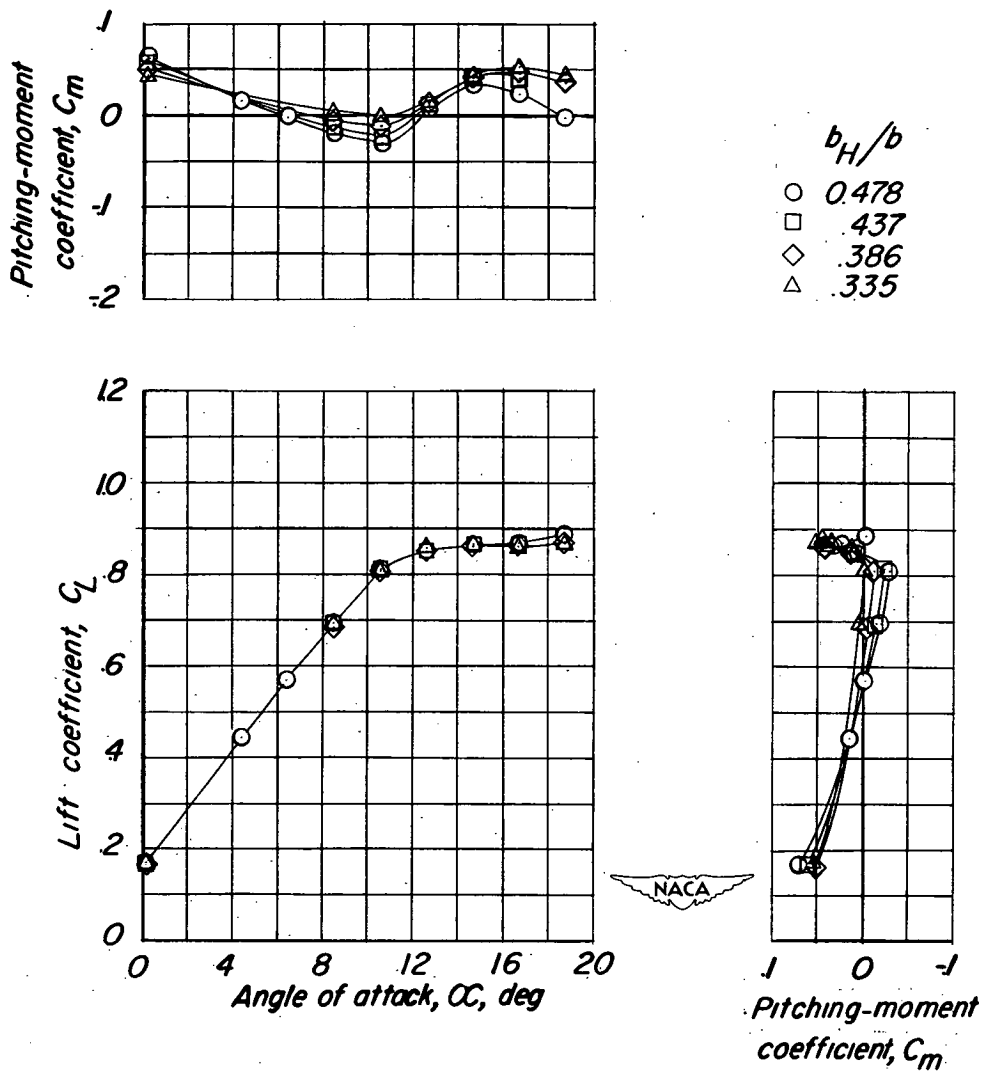


Figure 17.- Effect of horizontal-tail span on aerodynamic characteristics in pitch of a  $35^\circ$  swept-wing model.  $\delta_f = 0^\circ$ .

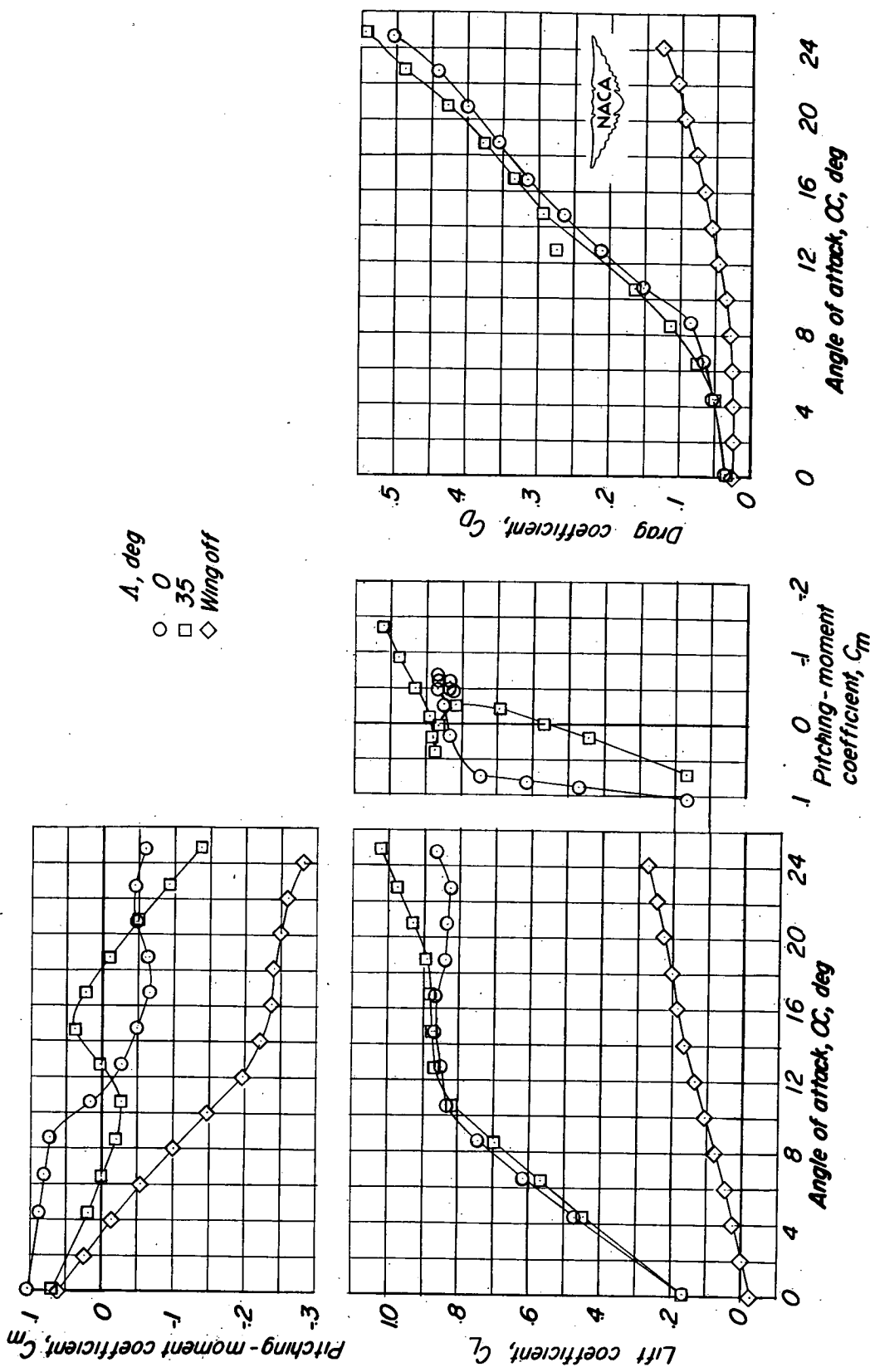


Figure 18.- Effect of wing sweep on aerodynamic characteristics of a model having swept tail surfaces.  $\delta_F = 0^\circ$ .  $A = 3.57$ .

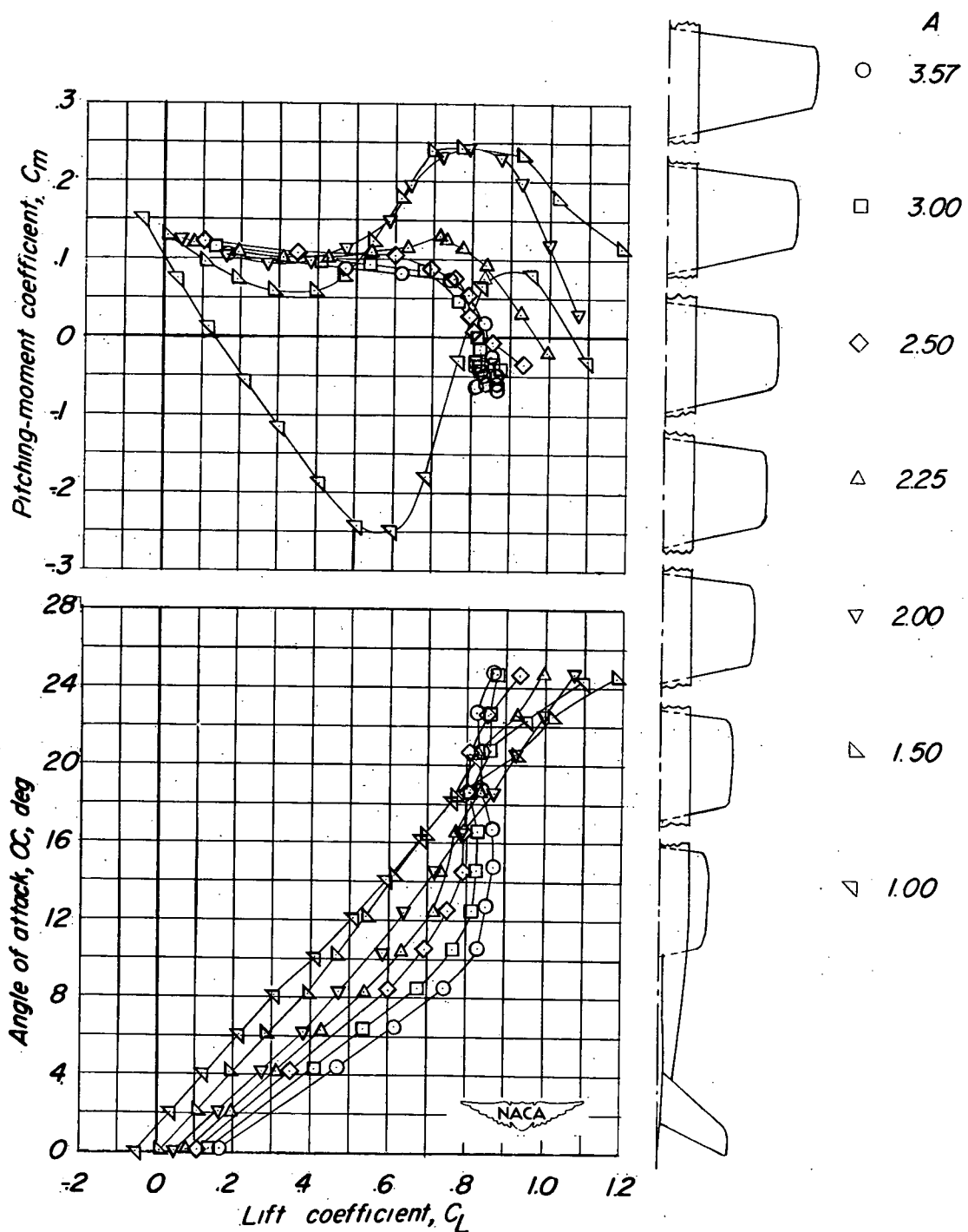
(a) Variation of  $C_m$  and  $\alpha$  with  $C_L$ .

Figure 19.- Effect of aspect ratio on the aerodynamic characteristics in pitch of a complete model having an unswept wing and swept tail surfaces.  $\delta_f = 0^\circ$ .

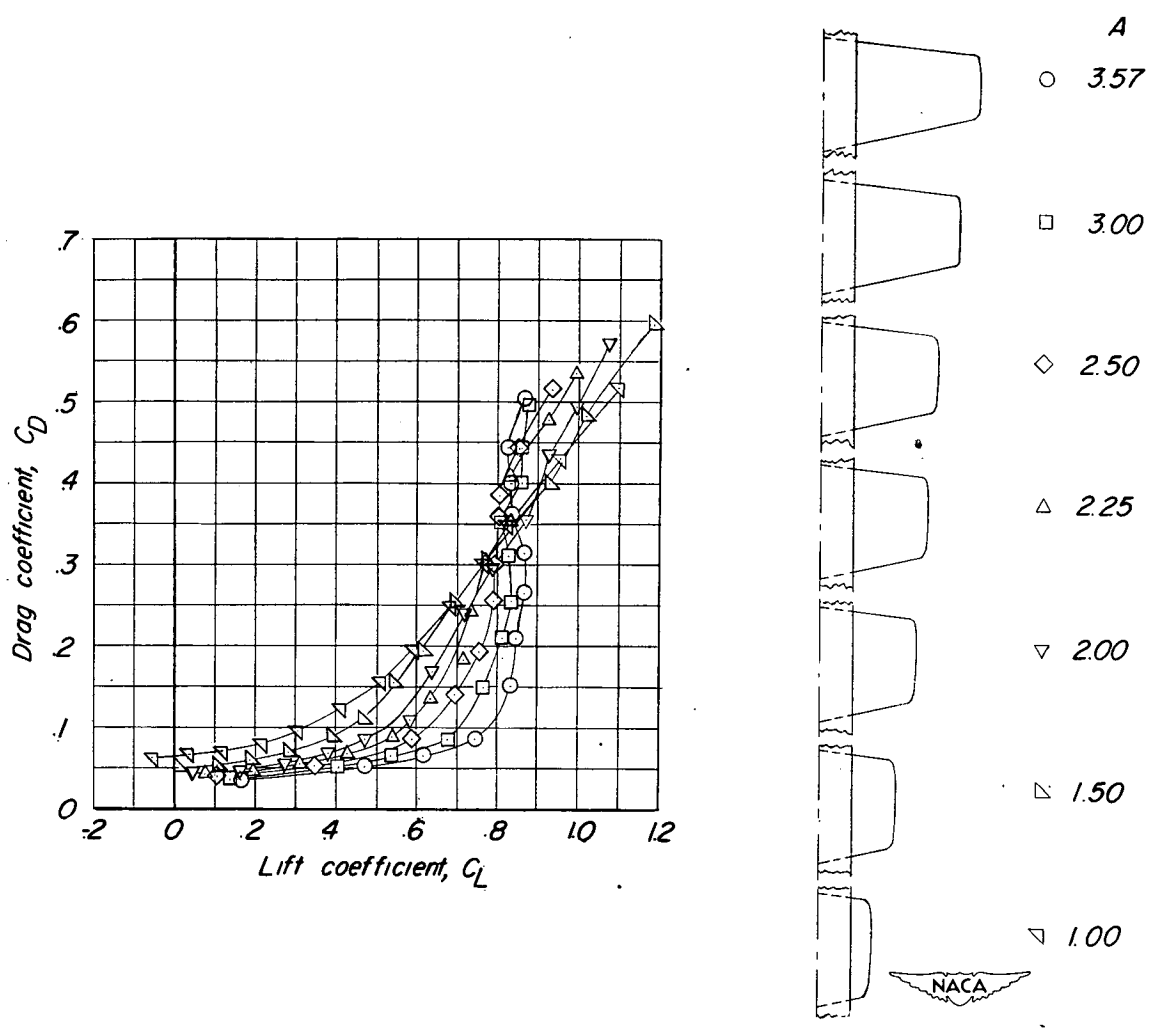
(b) Variation of  $C_D$  with  $C_L$ .

Figure 19.- Concluded.

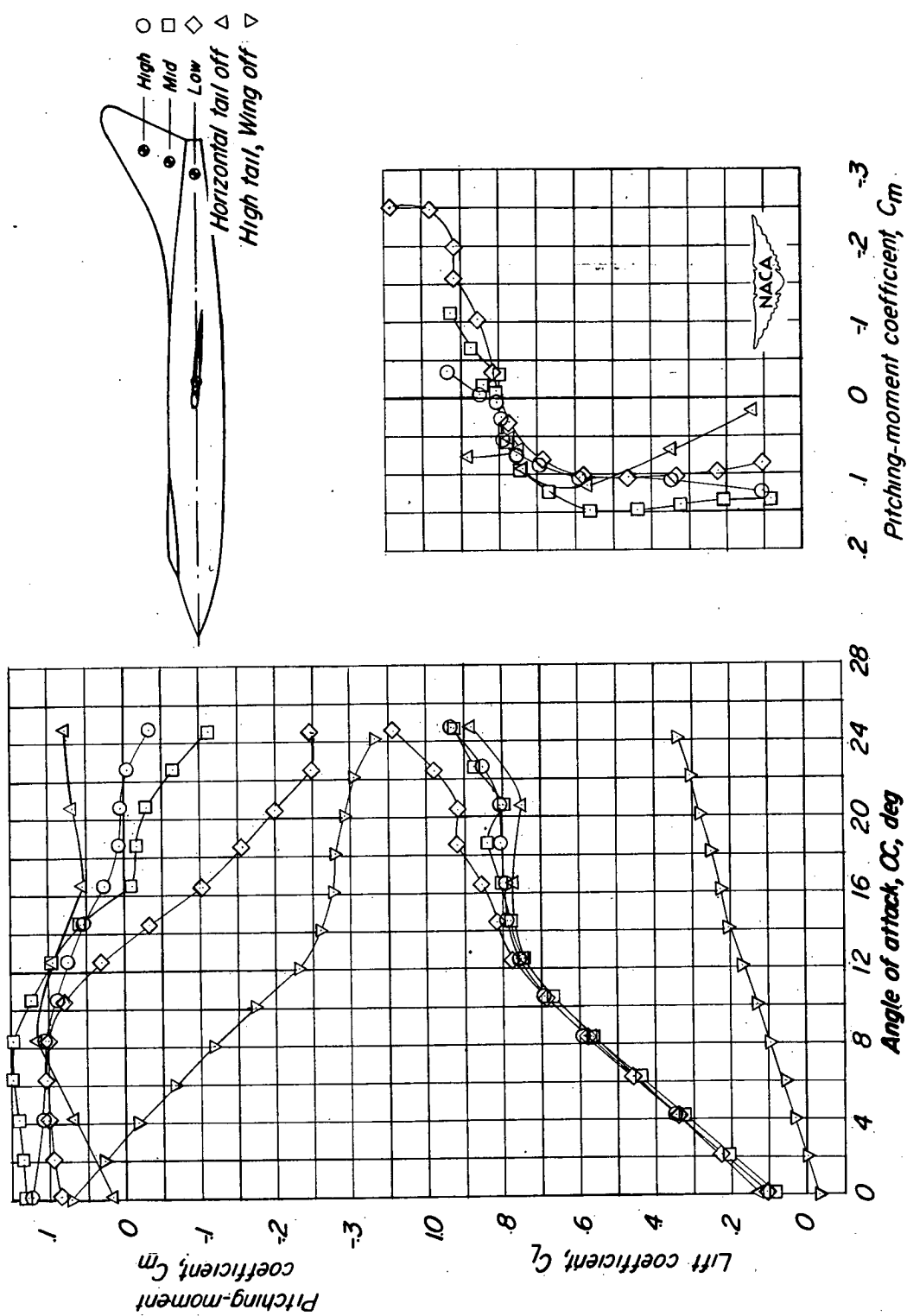
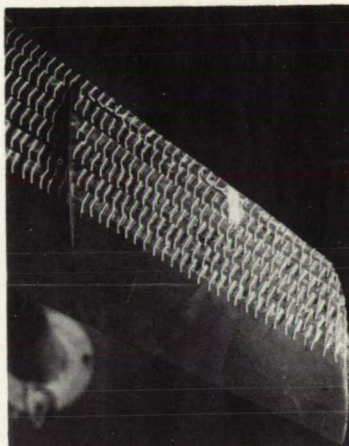


Figure 20.- Effect of horizontal-tail position on aerodynamic characteristics in pitch of an unswept-wing model.  $A = 2.50$ .  $\delta_f = 0^\circ$ .

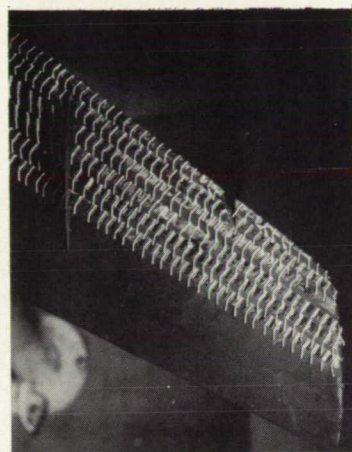
Original wing

 $\alpha_c$   
(deg)

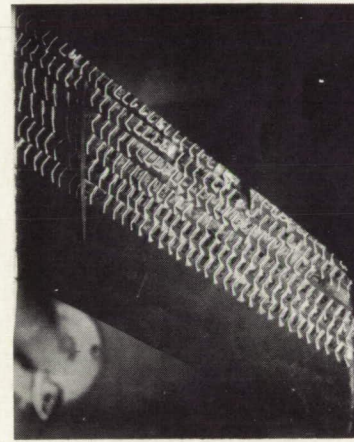
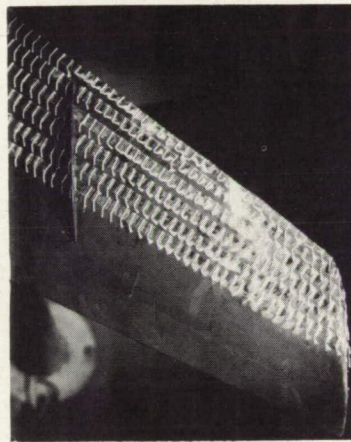
4



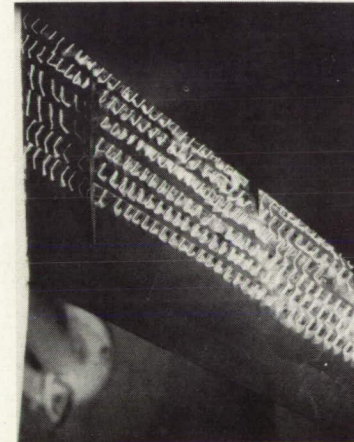
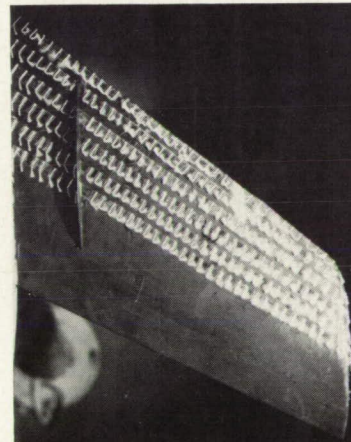
0.02 b/2 notch at 0.74 b/2



8



12



L-80300

Figure 21.- Surface tuft photographs for the original wing and notched wing arrangements. Reynolds number,  $0.885 \times 10^6$ .

~~SECURITY INFORMATION~~

~~CONFIDENTIAL~~

~~CONFIDENTIAL~~